Agriculture, Ecosystems and Environment 399 (2026) 110179

Contents lists available at ScienceDirect

Agriculture, Ecosystems and Environment

journal homepage: www.elsevier.com/locate/agee

From roots to residues: Tracing contrasting pathways of carbon incorporation into soil organic matter of a Mediterranean agricultural trial

Layla M. San-Emeterio [a,*], Ian D. Bull [b], Jens Holtvoeth [c], Rafael López-Núñez [d], José A. González-Pérez [d]

[a] Department of Soil and Environment, Swedish University of Agricultural Sciences (SLU), Lenmart Hjelms Väg 9, P. O. Box 7014, Uppsala 75007, Sweden
[b] Organic Geochemistry Unit, School of Chemistry, University of Bristol, Cantocks Close, Bristol BS8 1TS, United Kingdom
[c] School of Health & Life Sciences, Teesside University, Middlesbrough TS1 3BX, United Kingdom
[d] Instituto de Recursos Naturales y Agrobiología de Sevilla (IRNAS-CSIC), Avenida Reina Mercedes 10, Sevilla 41012, Spain

ARTICLE INFO

Keywords:
Soil carbon
Biomarkers
Vegetation change experiments
Stable carbon isotopes
Compound specific isotope ratios

ABSTRACT

Mediterranean agricultural soils are characterized by low organic matter content and high mineralization rates, making carbon stabilization a particular challenge. Here, we combined lipid biomarker analysis with compound-specific stable isotope analysis (CSIA) to trace the incorporation of maize-derived C following a crop switch from wheat (C_3) to maize (C_4). Two treatments were compared: (A) biomass+root inputs and (B) root-only inputs. Within 21 months, significant enrichment in $\delta^{13}C$ was detected across compound classes, with long-chain *n*-alkanes, hydroxy acids and sterols showing increases of + 3 to + 6 ‰, especially in the upper 5 cm, while unsaturated fatty acids displayed minor contributions (< 1 ‰) due to rapid turnover. Aboveground residue inputs (treatment A) enhanced microbial assimilation of maize carbon in surface soils, leading to fast but short-lived incorporation, consistent with shorter bulk SOC mean residence times (MRT) of ca. 15 days compared to the root-only treatment (ca. 28 days). In contrast, root-derived inputs (treatment B) contributed to more persistent pools at depth, where bulk SOC MRTs increased up to 30 days and suberin-derived biomarkers showed pronounced environment. Bulk SOM $\delta^{13}C$ showed smaller changes (< 1 ‰) than individual compounds, underscoring the value of CSIA for capturing short-term dynamics. These results demonstrate the complementary roles of aboveground residues and roots in shaping SOC turnover and stabilization. In Mediterranean soils with inherently low organic matter stability, residue management strongly mediates both the amount and persistence of new carbon, with implications for developing residue-management strategies that enhance potential pathways towards carbon stabilization in fragile Mediterranean agroecosystems.

1. Introduction

Soil organic matter (SOM) is central to terrestrial carbon (C) cycling and climate regulation, yet its persistence remains highly variable and context-dependent. The chemical heterogeneity of SOM arises from the continuous input of plant and microbial residues and their subsequent transformations in soils. Among SOM constituents, lipids are particularly informative because they include both plant waxes and microbial membrane components that act as biomarkers for sources and processes (Wiesenberg et al., 2004; Hirave et al., 2020). Their variable stability, from resistant long-chain *n*-alkanes to labile fatty acids and alcohols, makes them valuable tracers of decomposition and stabilization pathways (Tu et al., 2017; Lv et al., 2022). Mediterranean agricultural soils are especially relevant in this context, as they are characterized by low SOM content, high mineralization rates, and vulnerability to degradation under intensive cultivation (Francaviglia et al., 2018; Ferreira et al., 2024).

A key unresolved question is the relative contribution of above- versus belowground plant inputs to soil organic carbon (SOC) persistence. Aboveground residues are typically more labile, rapidly decomposed at the soil surface, and strongly coupled to short-term microbial activity (Fanin and Bertrand, 2016). In contrast, root-derived inputs penetrate deeper into the profile and are enriched in biopolymers such as suberin that are more resistant to decomposition, thereby contributing disproportionately to long-term SOC stabilization (Crow et al., 2009; Angst et al., 2018; Sokol and Bradford, 2019). Recent syntheses

* Corresponding author.
E-mail address: layla.marquez.san.emeterio@slu.se (L.M. San-Emeterio).

https://doi.org/10.1016/j.agee.2025.110179
Received 30 September 2025; Received in revised form 26 November 2025; Accepted 17 December 2025
Available online 2 January 2026

suggest that belowground inputs may dominate SOC formation (Fu et al., 2025), yet field-based evidence disentangling the fate of roots and aboveground residues under different management strategies remains scarce, particularly in Mediterranean croplands. However, there is a notable lack of field-based studies that use compound-specific isotope analysis (CSIA) of diverse lipid biomarkers to disentangle how these two above- versus belowground residue-derived carbon is incorporated and transformed in Mediterranean soils.

Stable isotope approaches provide a powerful means to trace plant carbon into soils. The natural difference in $\delta^{13}C$ between C_3 and C_4 plants creates an in-situ tracer for following new organic matter inputs (Balesdent and Mariotti, 1996; Wynn and Bird, 2007). Crop-switching experiments exploit this shift to estimate SOC turnover and the routing of new C into different pools. This abovementioned CSIA approach further enhances this approach by resolving isotopic changes in individual biomarker classes, which may be masked at the bulk level (Reiffarth et al., 2016; Smith and Chalk, 2021). Combined with molecular proxies such as carbon preference index (CPI) and average chain length (ACL), CSIA enables a detailed assessment of how distinct plant fractions contribute to SOM formation (Ren et al., 2016).

Here, we apply a C_3– C_4 crop-switching experiment in Mediterranean soils, replacing wheat (C_3) with maize (C_4) and applying two residue management treatments: (i) retention of roots only (*root*), and (ii) retention of both roots and chopped aerial biomass (*biomass+root*). This design allows us to disentangle the pathways of maize-derived carbon incorporation into bulk SOC and lipid biomarkers. We hypothesized that (1) overall SOC accumulation would remain low due to the high mineralization potential of Mediterranean soils; (2) incorporation of maize-derived C would be greater in surface soils due to intense microbial activity and faster turnover in the upper horizons; and (3) aboveground residue addition would primarily enhance rapid maize-derived C incorporation into labile pools at the surface, whereas root-only inputs would contribute more persistently to deeper SOM stabilization through suberin-rich tissues and rhizodeposition.

2. Materials and methods

2.1. Study area and experimental setup

This experiment was carried out at the "La Hampa" experimental farm belonging to the "Instituto de Recursos Naturales y Agrobiología de Sevilla (IRNAS-CSIC)". The farm is located in the municipality of Coria del Río, Seville (Spain) (37°16'54"N, 6°03'47"W) under a typical Mediterranean climate. From the farm's agroclimatic station the average temperature during the duration of the experiment was 12.2 °C during winter (month to month) and 25.8 °C during the spring-summer season (month to month), with mild rainy winters (496 mm mean annual rainfall;). The soil, a Calcaric Cambisol with a sandy clay loam texture (IUSS Working Group WRB, 2014), is characterised by high carbonate content (~27 %), low fertility and low organic matter content (~1.5 %).

The experimental trial consisted of a crop switching experiment, entailing the tracing of carbon using the C_4 biosynthetic pathway, where maize discriminates less strongly against ^{13}C, i.e., $\delta^{13}C$ values of SOM and fatty acids originating from maize are expected to be less negative than those of fatty acids from wheat. The experimental design consisted of a factorial field study with a completely randomized block design (Fig. 1), where, from February 2017 a wheat crop (*Triticum aestivum* L., C_3 plant) was replaced by a maize (*Zea mays* L.) crop (C_4 plant), comprising two treatments in two plots each: (A) after harvesting, maize aerial parts were chopped and applied to the surface soil, besides leaving the roots and hereafter designated as 'biomass+root' treatment; (B) the total part of maize plant was left out after harvesting leaving the roots, hereafter known as the 'root' treatment. Each treatment was applied to two sub-replicate plots of approximately $10 \times 0.75 \times 4 = 30\ m^2$, with a separation distance of 0.75 m, resulting in a total of four plots. Additionally, control samples were collected from two separate plots (sub-replicates) adjacent to the treatment plots within the same field. This control soil was tilled but not planted with maize, and therefore retained the same isotopic signature as the soil under its former land use (C_3 vegetation). The experimental area covered approximately 2500 m^2.

2.2. Soil sampling and preparation

Soil sampling was conducted in November 2018, 21 months after the experiment's inception. From each plot, a composite soil sample was taken, consisting of three sub-samples combined at each of the three different depths: 0–5, 5–20 and 20–40 cm. In total, 18 soil samples were taken. Soils were oven-dried at 40 °C for 3 days then roughly ground using a mortar and pestle and dry sieved through a sieve < 2 mm; macroscopic plant remains, and stones were removed with tweezers.

Prior to carbon content and bulk stable isotope analysis, carbonates that may interfere with elemental SOC and stable carbon isotope ($\delta^{13}C$) analysis were removed by direct acidification with 1 M HCl following

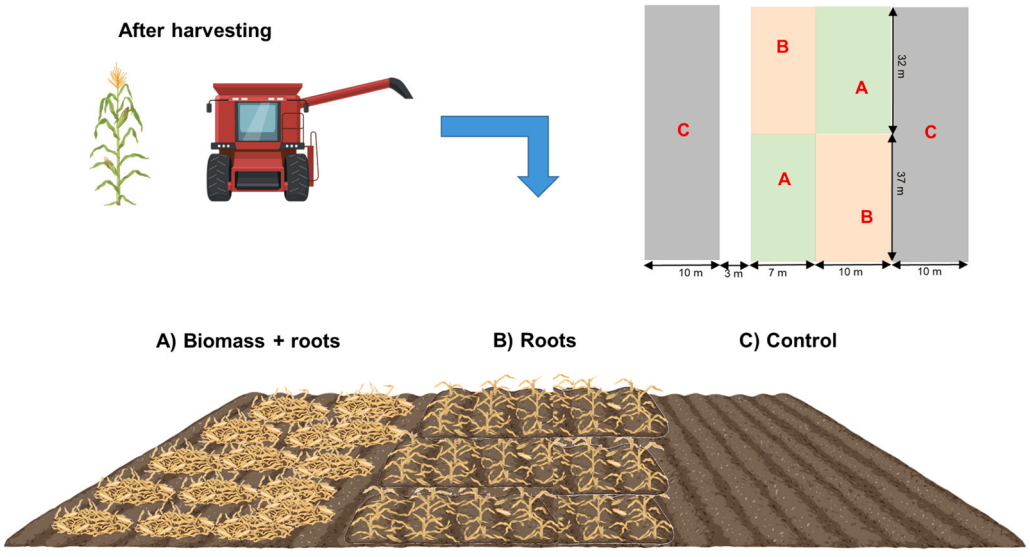

Fig. 1. Experimental layout of the C_3 to C_4 vegetation change trial, illustrating the two treatments (A: biomass+root; B: root-only), their replicated plots, and the adjacent control plot maintained under the original C_3 vegetation.

Verardo et al. (1990). Carbonates were removed by, and samples were not exposed to acid for more than 6 h to avoid preferential loss of ^{13}C-enriched organic moieties during decarbonation, as prolonged acid treatment can slightly alter $\delta^{13}C$ values (Komada et al., 2008).

2.3. Elemental and bulk isotopic composition of soil

For $\delta^{13}C$ bulk isotopic determinations, 2.5 mg aliquots of bulk soil samples were weighted into tin capsules. Each soil sample was analysed in duplicate ($n = 2$) to ensure measurement precision, representing technical replicates. The analysis was performed using an EA IsoLink™ IRMS System (Thermo Fisher Scientific, Bremen, Germany). The EA microanalyzer was equipped with a combustion furnace set at 1020°C and coupled *via* a ConFlo IV interface unit to a continuous flow Delta V Advantage isotope ratio mass spectrometer (IRMS) for measuring $\delta^{13}C$ values. Isotopic values were corrected by using appropriate standards recognized by the International Atomic Energy Agency (IAEA).

The stable isotope determinations are reported in the delta (δ) notation (e.g., $\delta^{13}C$) relative to an international measurement standard. The isotope value is defined in Coplen (2011), according to Eq. (1).

$$\delta^{13}C_{sample} = \frac{R \quad (\delta^{13}/\delta^{12})sample}{(\delta^{13}/\delta^{12})standard} - 1 \tag{1}$$

Where "R" is the molar ratio of the heavy (^{13}C) to light (^{12}C) most abundant isotope of carbon. The "δ" values are reported in per mil (‰). The stable isotope standard for reporting carbon measurements is the Vienna Pee Dee Belemnite limestone (VPDB scale). The analytical precision and accuracy of bulk $\delta^{13}C$ values was typically less than ± 0.5 standard deviation. The total C was determined by the dry combustion method using the same instrument specified above (EA IsoLink) in the CN analyser mode.

2.4. Total lipid extraction (TLE)

Soil lipids were extracted from each soil sample (7 g) in a solvent mixture of dichloromethane and methanol (3:1 (for 45 min), using a microwave-assisted extraction system (Ethos, EX, Milestone, Italy), heating the samples to 70 ºC at 5 ºC/min and holding the temperature for 10 min. The total lipid extract (TLE) was then concentrated through evaporation and passed through sodium sulphate (anhydrous) to remove any remaining water. Fatty acids in the TLE were transmethylated by adding 1 ml of MeOH:acetyl chloride (30:1), left to react for 12 h at 45°C to form GC-amendable fatty acid methyl esters (FAMEs). The extracts were then passed through potassium carbonate, which removes excess acid (acetic acid, hydrochloric acid). Compounds containing hydroxy groups (e.g., hydroxy acids, alcohols, sterols) were silylated using N,O-bis-(trimethyl-silyl)-trifluoroacetamide (BSTFA, with 1 % trimethyl-chlorosilane), kept at 65 °C for 30 min.

Compounds were first screened by gas chromatography with flame ionization detection (GC-FID) and, subsequently, by gas-chromatography-mass spectrometry (GC-MS). The GC-MS analyses were carried out using a Trace 1300 Series gas chromatograph (GC) fitted with a HP-1 non-polar capillary column (50 m × 0.32 mm i.d., 0.17 μm film thickness; carrier gas: helium at 2.00 ml min^{-1}; on-column injector). The GC oven temperature was programmed from 60 ºC to 170 ºC at 6 ºC min^{-1}, then to 315 ºC at 2.5 ºC min^{-1} and held for 10 min. The column was fed directly into a single quadrupole mass spectrometer model ISQ-LT (Thermo Fisher Scientific, Waltham, MA, USA). Organic compounds were identified through their mass spectra and their relative retention times. All compounds were quantified by comparing their peak area to the peak area of an internal standard (5α-cholestane). A known volume and concentration of the standard (100 μL of a 124.2 ng μL^{-1}) was added to each sample prior to extraction to correct for losses throughout the entire analytical procedure.

2.5. Compound-specific isotope analysis (CSIA)

Compound-specific carbon isotope compositions of selected biomarkers were measured with a Finnigan Trace gas chromatograph coupled to a Finnigan Delta XP isotope ratio mass spectrometer (GC-C-IRMS) (Thermo Scientific, Hamburg, Germany) equipped with a DB-5MS column (60 m × 0.25 mm internal diameter, film thickness 0.25 μm). Aliquots (1 μL) of TLE were injected in splitless mode at an injector temperature of 300 °C. The GC oven temperature was programmed from 50 °C (held for 1 min) to 220 °C at a rate of 10 °C min^{-1} (held for 2 min) and then to 300 °C at a rate of 2 °C min^{-1} (held for 20 min), and finally to 310 °C at a rate of 10 °C min^{-1} (held for 20 min). Helium was used as the carrier gas (1.4 ml min^{-1}). Instrument performance was verified before and after each sample run using a FAME standard mixture (C_{11}, C_{13}, C_{16}, C_{21}, and C_{23} FAME) with known $\delta^{13}C$ values ranking from –31.58 to –28.83 ‰ (Sigma-Aldrich, U.S.A.). Reproducibility of the $\delta^{13}C$ values for specific compounds (i.e., *n*-alkanes) was better than ± 0.5 ‰ (standard deviation), based on triplicate analyses ($n = 3$). Results are reported in the δ notation (‰) relative to the Vienna Peedee Belemnite (VPDB) standard.

2.5.1. Mass balance correction

The $\delta^{13}C$ values of fatty acid methyl esters (FAMEs) were corrected for the exogeneous carbon added during the methylation process (from methanol: –44.74 ‰) according to the mass balance equation of Rieley (1994):

$$n_{cd}\delta^{13}C_{cd} = n_c\delta^{13}C_c + \quad n_d\delta^{13}C_d \tag{2}$$

where *n* is the number of C atoms, *c* the underivatized compound, *d* the derivatising agent and *cd* is the derivatised compound.

2.5.2. Calculations of new carbon and turnover times of specific compounds

The introduction of C_4-cropping on previously exclusively C_3-cropped soils allows for calculation of new C_4-incorporations. Turnover time calculations are based on turnover rates under assumed steady state conditions, i.e., the carbon content (net balance of input and degradation) is constant in the soils (Balesdent and Mariotti, 1996). The incorporation of new carbon by C_4-vegetation (f_{C4}) can be calculated as follows (Balesdent et al., 1987):

$$f_{C4} = \frac{\delta^{13}C_{C4soil} \quad - \delta^{13}C_{C3soil}}{\delta^{13}C_{plant} \quad - \delta^{13}C_{C3soil}} \tag{3}$$

where $\delta^{13}C_{plant}$ is the isotope composition of C_4- plant (maize), according to the 'A' and 'B' treatment plots. $\delta^{13}C_{C4\ soil}$ and $\delta^{13}C_{C3\ soil}$ are the isotope composition of the C_4-cropped soil and the original C_3-cropped soil. Then, the SOC decomposition is assumed in most models to follow a first-order kinetics at steady state conditions (Balesdent and Mariotti, 1996). The decomposition of SOC per time unit was introduced as turnover rate equivalent to the decay rate or decomposition rate (*k*) can be calculated (Collins et al., 1999) as:

$$k = \frac{\ln(1 - f_{C4})}{t} \tag{4}$$

Where *t* is the time at which soils were sampled since the experiment was firstly established. Based on this calculation the turnover time rate (*k*), which is used synonymously to the mean residence time (MRT) of organic carbon in soils, can be calculated as:

$$MRT = \quad 1/k \tag{5}$$

To study the new maize proportions and turnover times of bulk soils and individual lipid fractions we applied the equations given above to each, bulk SOC, and those individual compounds that were identified by CSIA.

2.6. Diagnostic biomarker distributions and proxies

Lipids are frequently used to calculate diagnostic ratios, which are than related to SOC sources and dynamics. These compounds can also be used to trace microbial activity (Xie et al., 2004, Andersson et al., 2011). Presence of specific biomarkers, their diagnostic distributions and ratios, and conclusions that can be drawn from these are briefly discussed henceforth.

2.6.1. n-alkanes

n-Alkanes are used to calculate the Carbon Preference Index (CPI_{ALK}), reflecting the degree of odd-over-even predominance for *n*-alkane chain lengths. The CPI_{ALK} can indicate inputs of plant-derived organic matter since leaf waxes of higher plants have a strong odd/even predominance (CPI > 10) or to which degree this material has been degraded, mainly by bacteria (CPI values close to 1). Here, the CPI index was calculated for *n*-alkanes with 24–31 carbon atoms, using a modified formula from Cranwell (1973) as described in San-Emeterio et al. (2023a):

$$CPI_{ALK} = \left[\left(\sum C_{25-33}odd \Big/ \sum C_{24-32}even\right) + \left(\sum C_{25-33}odd \Big/ \sum C_{26-32}even\right)\right] \Big/ \quad 2 \tag{6}$$

where C_n *odd* and C_n *even* are the abundances of *n*-alkanes with odd-numbered and even-numbered carbon chains, respectively.

The hydrocarbon average chain length (ACL) index can be used as a proxy for the source and degradation of SOM (Gonzalez-Vila et al., 2003). It can be used to identify the source of organic matter, from microbial-derived or reworked organic matter, characterised by a shorter ACL, to fresh plant-derived organic matter with higher ACL values, with long-chain homologues (carbon number ≥ 26) typically deriving from leaf waxes (Bush and McInerney, 2013 and references therein). While ACL values of long-chain hydrocarbons are not chemotaxonomically diagnostic in general, shifts in ACL may still indicate changes in specific organic matter sources, in particular, if the sources can be narrowed down and/or the ACL of potential sources are known (e.g., Holtvoeth et al., 2016). ACL was calculated for the long *n*-alkane range (C_{26-33}):

$$ACL = \sum(C_n \times n)_{26-33} \Big/ \sum(C_n)_{26-33} \tag{4}$$

where n is the number of carbon atoms and C_n is the relative abundance of the respective alkane with n carbons.

The short-over-long chain length ratio (S/L) is the relative abundance of short to long hydrocarbon chains. S/L was calculated according to the following Eq. (5):

$$S \Big/ L = \sum(C_n)_{10-23} / (C_n)_{24-32} \tag{7}$$

where n is the number of carbons and C_n is the relative amount of the respective alkane with n carbons.

2.6.2. n-alkanols

Saturated C_{22-30} *n*-alkanols in plants show a strong even-over-odd predominance. In analogy to the *n*-alkanes, variation of this dominance can provide information about SOM degradation and can be calculated as CPI_{OH} as suggested by Routh et al. (2014):

$$CPI_{OH} = \frac{\sum C_{20-26}even + \sum C_{22-28}even}{2 \times \sum C_{21-29}odd} \tag{8}$$

It should be noted that this equation includes the mid-chain C_{22} and C_{24} *n*-alkanols, which in soils can derive from suberin in root tissue rather than leaf waxes (Holtvoeth et al., 2016).

The Higher Plant Alkane (HPA) index was introduced by Poynter and Eglinton (1990) to provide a numerical measure of degradation of non-functionalised *vs*. functionalised compounds: where alkanols and alkanoic acids are susceptible to microbial degradation, *n*-alkanes tend to be selectively preserved. This can be expressed by the HPA index, calculated according to Routh et al. (2014):

$$HPA = \frac{(C_{24} + C_{26} + C_{28})alkanol}{(C_{24} + C_{26} + C_{28})alkanol + \quad (C_{25} + C_{27} + C_{29})alkane} \tag{9}$$

2.6.3. n-alkanoic acids

Like *n*-alkanols, *n*-alkanoic acids (saturated fatty acids) from plant sources feature a strong even-over-odd predominance. In order to cover two main distinct sources (microbial biomass and plants, the carbon preference index for fatty acids, CPI_{FA}, was calculated comprising two ranges: short-chain FAs of bacterial origin (C_{12}-C_{22}) (Eq. 10), and long-chain FAs (C_{23}-C_{32}) (Eq. 11):

$$CPI_{short-FA} = \left[\left(\sum C_{12-22}even \Big/ \sum C_{13-19}odd\right) + \left(\sum C_{12-22}even \Big/ \sum C_{15-21}odd\right)\right] \Big/ \quad 2 \tag{10}$$

$$CPI_{long-FA} = \left[\left(\sum C_{24-32}even \Big/ \sum C_{23-29}odd\right) + \left(\sum C_{24-32}even \Big/ \sum C_{25-31}odd\right)\right] \Big/ \quad 2 \tag{11}$$

2.7. Statistical analysis

Normality and homoscedasticity were checked prior to all the analyses using the Kolmogorov-Smirnov test and the Levene test, respectively. In those cases where data did not meet the normality or homogeneity requirements a log transformation was applied before further analysis. In the cases where the normality and homoscedasticity requirements were met, an analysis of variance (ANOVA) and a multiple comparison test (Tukey) was made. In cases these requirements were not met, non-parametric tests were completed, i.e., the Kruskal-Wallis test along with a Dunn post-hoc test for multiple non-parametric comparisons, and the Mann-Whitney *U* test. These statistical analyses were made with a 95 % confidence level using the statistical package SPSS 20.0 (SPSS Inc., Chicago, USA).

Table 1
Soil parameters corresponding to the different plots and treatments, at different soil depths (mean ± SE, n = 4).

Treatment	Depth (cm)	pH	SOC (%)	$\delta^{13}C$ bulk (‰)	$CaCO_3$ (%)	TLE (μg g^{-1} SOC %)
Biomass + roots, 'A'	5	8.5 ± 0.1	0.82 ± 0.07^{b}	−24.0 ± 0.3^{a}	27.2 ± 0.2	46.6 ± 5.2
	20	8.5 ± 0.1	0.77 ± 0.05^{b}	−24.8 ± 0.2^{a}	26.8 ± 0.7	49.7 ± 2.5
	40	8.9 ± 0.3	0.41 ± 0.07^{a}	−24.1 ± 0.2^{a}	27.6 ± 0.3	24.3 ± 5.0
Roots, 'B'	5	8.7 ± 0.1	0.85 ± 0.04^{b}	−24.5 ± 0.3^{a}	24.5 ± 2.8	53.8 ± 3.2
	20	8.9 ± 0.0	0.83 ± 0.04^{b}	−24.4 ± 0.2^{a}	26.8 ± 1.1	54.0 ± 4.4
	40	9.1 ± 0.1	0.66 ± 0.11^{a}	−24.5 ± 0.2^{a}	28.0 ± 0.5	37.2 ± 2.6
Control	5	8.2 ± 0.0	1.1 ± 0.0^{b}	−25.8 ± 0.2^{b}	25.3 ± 0.8	45.9 ± 1.4
	20	8.3 ± 0.1	0.91 ± 0.09^{ab}	−25.8 ± 0.2^{b}	25.9 ± 0.8	33.9 ± 6.0
	40	8.3 ± 0.1	0.74 ± 0.02^{a}	−24.8 ± 0.0^{b}	25.6 ± 0.9	22.4 ± 0.3

TLE: Total lipid extract. Significant differences ($p < 0.05$) are indicated by different letters between depths for the same treatment.

3. Results

3.1. Soil organic carbon and bulk $\delta^{13}C$ patterns

The elemental data from the soil samples is summarized in Table 1. Accordingly, SOC contents display a pattern with higher contents in the upper subsoil and significantly lower contents at a depth of 40 cm ($p < 0.05$). No differences were observed in either pH values or carbonate content, either between treatments or down the soil profile. Significant differences are observed for the bulk $\delta^{13}C$ values, which are more depleted in the control plots compared to the treatments, whilst no effects of the depth are observed.

Total lipid extracts (TLEs) are given as μg related to SOC content (Table 1). The TLE concentration did not differ in soil from the treatment and control plots ($p = 0.193$). The decrease of TLE concentration with depth ($p = 0.032$), reflecting a normal pattern as lipids become more degradable than the SOC.

3.2. Lipid analysis

The TLEs from all soil samples were found composed of homologous series of short-chain ($< C_{22}$), mid-chain (C_{22}-C_{24}) and long-chain ($> C_{24}$) fatty acids (FAs), branched and unsaturated FAs (both mono- and polyunsaturated), α- and ω- hydroxy FA, *n*-alkanols, *n*-alkanes, and sterols. A detailed list of all quantified compounds is provided in Table S1, along with a selection of major compounds sorted by their biogenic groups (Table S2), and an example chromatogram is shown in Fig. 2. Short-chain and monounsaturated FAs (MUFAs) were the predominant compounds in the TLEs. The MUFAs ($C_{n:1}$, namely various isomers of $C_{16:1}$, $C_{18:1}$, $C_{20:1}$ and $C_{22:1}$) were also detected in remarkable amounts in all samples (71.6–237.9 μg g^{-1} SOC-TLE; Table 1).

3.2.1. n-alkanes

The chain-length distribution of *n*-alkanes ranged from C_{16} to C_{33}, with maximum at C_{29} and C_{31} (Fig. 3a; Table S2). Overall abundances were lower in control compared to both maize treatments. The CPI_{ALK} values ranged from 2.1 to 7.7 and were significantly higher at 5 cm in all plots, with an additional increase at 20 cm in the root-only treatment (B) ($p < 0.01$; Fig. 4a). ACL values varied between 29.2 and 30.7, with no significant treatment effects ($p > 0.05$). Depth-related increases in ACL were significant in the control plots (0–20 cm) but not in the treatments, while lower values were found at 40 cm ($p < 0.05$; Fig. 5a). The S/L ratio was significantly higher at 40 cm than at 5 cm (0.75 ± 0.24 vs 0.40 ± 0.15; $p < 0.05$), except in treatment B where no depth effect was observed (Fig. 5b). Lastly, the HPA index ranged from 0.38 to 0.67, showing a significant decrease with depth in treatment B ($p < 0.05$; Fig. 5c).

3.2.2. n-Alkanols (saturated alcohols)

The *n*-alkanol distribution in all samples ranged from C_{12} to C_{32}, with a strong even-over-odd predominance and bimodal maxima at C_{18}–OH and $C_{28–30}$–OH (Fig. 3b). In the biomass+root (A) treatment, the relative abundance of C_{18}, C_{21}, and C_{26} homologues was significantly higher at 5 cm compared to the control ($p < 0.05$). No differences were observed at deeper depths. Treatment B showed intermediate abundances. The CPI index for alkanols (CPI_{OH}) ranged from 4.0 to 10.8, increasing significantly with depth in treatment plots, but not in controls ($p < 0.05$; Fig. 4b). This increase was accompanied by lower CPI_{ALK} values.

3.2.3. n-Alkanoic acids (saturated n-fatty acids)

The *n*-Alkanoic acids (FAs) constituted the highest proportion in all TLEs, with chain lengths ranging from C_{13} to C_{32} and showing a unimodal distribution peaking at C_{16} (Fig. 3c). Treatment plots contained significantly higher concentrations of short-chain FAs (C_{16}, C_{18}) in the top 20 cm compared to controls ($p < 0.05$). Long-chain FAs (C_{24}-C_{32}) were present across all plots, with mid-chain homologues (C_{22}, C_{24}) also detected. The CPI_{FA}-short ranged from 21.0 ± 1.3–44.7 ± 1.1, showing significantly lower values at 5–20 cm than at 40 cm in treatment plots ($p = 0.001$). No depth effect was observed in controls (Fig. 4c). The CPI_{FA}-long ranged from 2.0 ± 0.3–4.3 ± 0.1, with significantly higher values in treatments than in controls, particularly in topsoil ($p < 0.05$; Fig. 4d).

3.2.3.1. Mono- and poly- unsaturated fatty acids. MUFAs and PUFAs were detected in all samples, dominated by $C_{16:1}$ and $C_{18:1}$, along with minor $C_{20:1}$, $C_{22:1}$, $C_{24:1}$ and $C_{20:4}$ homologues (Table S1). Abundances were significantly higher in treatments compared to controls, particularly in the top 20 cm, with the biomass+root (A) plots showing elevated $C_{16:1cis9}$, $C_{18:1tr9}$, and $C_{20:3cis11}$ (Fig. 6a,b). In treatment B, two $C_{22:1}$ isomers were significantly more abundant at 40 cm ($p < 0.01$; Fig. 6c).

3.2.3.2. Branched fatty acids. Saturated branched FAs were identified in all soil samples within the C_{14}-C_{18} carbon range, in particular, the *iso*- and *anteiso*-branched forms of $C_{15:0}$ and $C_{17:0}$ FAs. In general, the

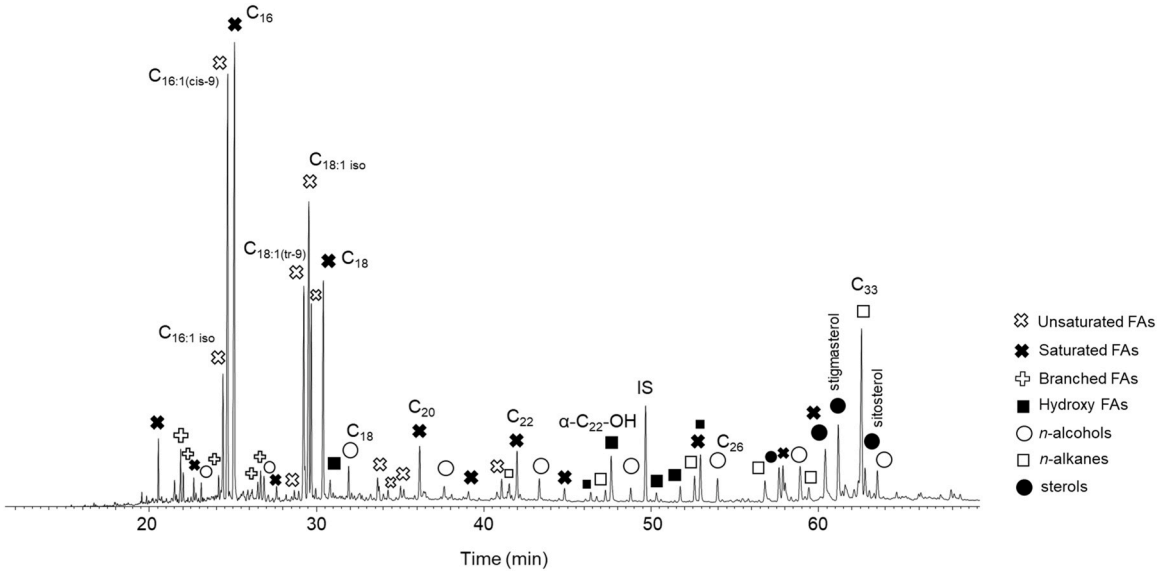

Fig. 2. Partial chromatogram of the total lipid extracts of a representative soil sample. Key: IS = internal standard (cholestane); C_{xx} refers to total carbon numbers.

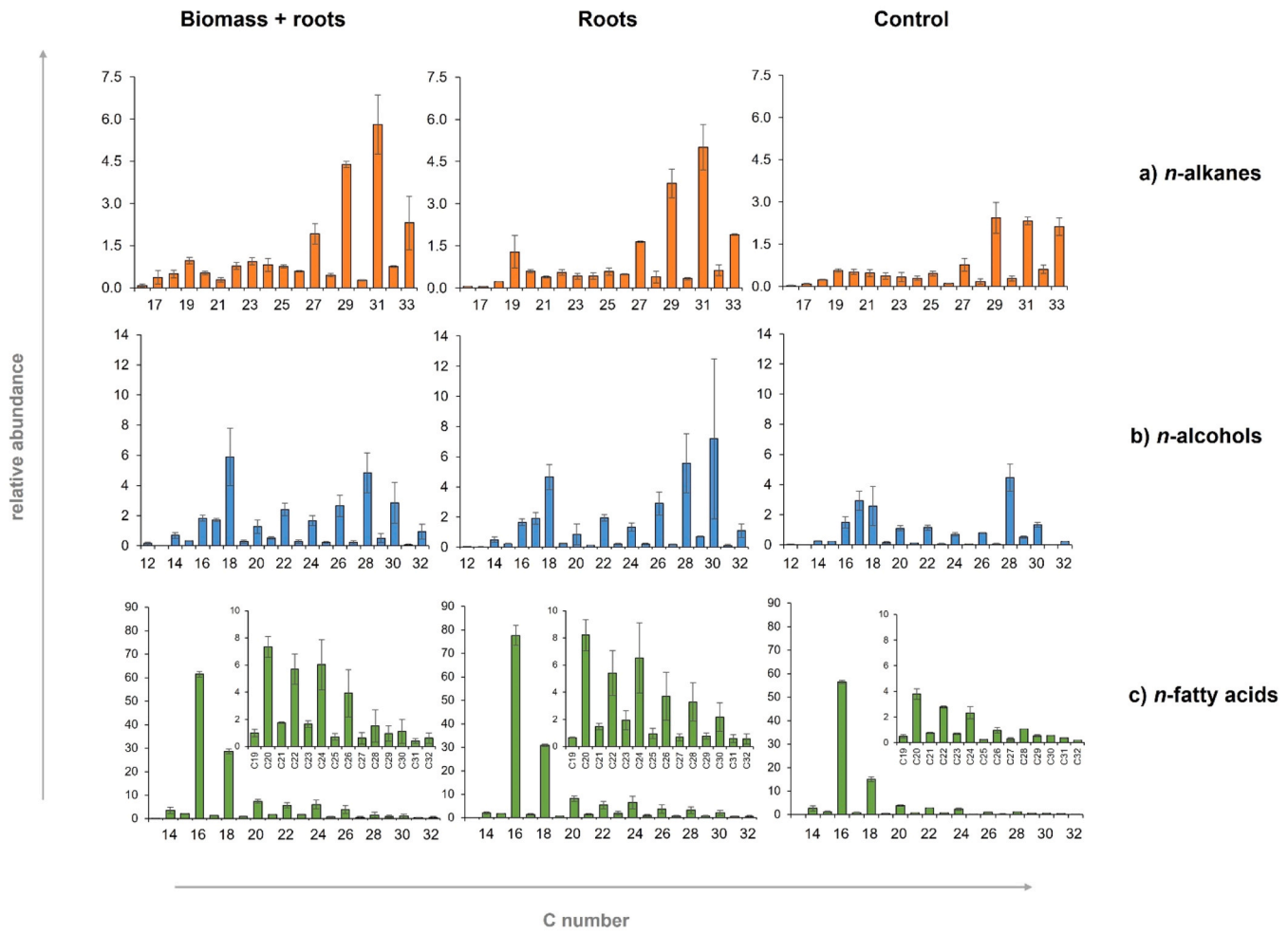

Fig. 3. Change-length distributions of a) n-alkanes, b) n-alcohols c) n-fatty acids (saturated) in soils under the three treatments. Values represent mean abundances (n = 4 ± standard error, SE) of each homologous compound, from the uppermost 5 cm which distribution is representative for all depths. Smaller bar graphs in c) show zoomed n-fatty acids chains.

presence of this group was significantly greater under both treatments compared to the control, with the exception of at 20 cm depth, where no significant differences were spotted. It is notable the remarkable influence of the 'B' treatment (only roots) at 40 cm in the abundance of this group of compounds pointing to high microbial activity (Fig. 6c). By looking at the specific compounds, the $C_{17:0}$ and C_{18} branched FAs were relatively more abundant in both treatments compared to the control. The presence of *i*-, *a*-$C_{15:0}$ branched FAs was notable under the "B" treatment ($p < 0.05$), leading to that increase at 40 cm that was mentioned above.

3.2.3.3. ω- and α- hydroxy acids. Hydroxy acids ranged from C_{15} to C_{24} and showed clear bimodal distributions. ω-hydroxy acids peaked at C_{16} and C_{24}, while α-hydroxy acids peaked at C_{16} and C_{22} (Fig. 7). In all cases, abundances were significantly lower in the control compared to the two maize treatments ($p < 0.05$). In the biomass+root (A) plots, α-C_{18} and short-chain α-$C_{15–16}$ homologues were relatively more abundant in the upper 5 cm. At depth (40 cm), ω-C_{22} and ω-C_{24} were more prominent in treatment plots, especially in the root-only (B) treatment.

3.2.4. Sterols

Five sterols were identified in the TLEs: cholesterol (C_{27}), campesterol (C_{28}), and stigmasterol, stigmastanol, and sitosterol (C_{29}) (Fig. 8). Sterol abundances were consistently lower in the control plots compared to both treatments. Among them, campesterol and stigmasterol were significantly more abundant in treatment soils ($p = 0.014$). Across all plots, sterol concentrations decreased with depth, with highest values in the top 5 cm.

3.3. Compound specific stable carbon isotope composition of lipids ($\delta^{13}C$ CSIA)

Reliable $\delta^{13}C$ values were determined for 21 compounds, including *n*-alkanes, *n*-alkanols, saturated and unsaturated fatty acids, hydroxy acids, and sterols (Table S3). Values ranged from –18.7 ± 0.3 to –38.1 ± 0.7 ‰, within the typical range for soil free lipids. Both maize treatments (A: biomass+root; B: root-only) showed systematic ^{13}C enrichment relative to the control, confirming the incorporation of C_4-derived carbon (Fig. 9). Bulk SOM $\delta^{13}C$ values were also enriched under maize, but to a lesser extent than individual compounds (Table 1), underscoring the higher sensitivity of compound-specific analysis. Importantly, the magnitude of this enrichment varied markedly across compound classes and between treatments, reflecting differences in biochemical origin and turnover.

Across all lipids, hydroxy acids and long-chain *n*-alkanes showed the strongest ^{13}C-enrichment, often exceeding that of fatty acids, alcohols, or sterols. In contrast, unsaturated fatty acids exhibited the smallest shifts, reflecting their rapid turnover. The identified *n*-alkanes (C_{27}, C_{29}, C_{31}), which were generally more depleted than other compound classes (mean values between –27.9 ± 0.4 and –35.9 ± 0.9 ‰), showed significant enrichment with treatment B exhibiting the strongest surface-layer ^{13}C signal ($p < 0.05$), consistent with greater contributions from root-

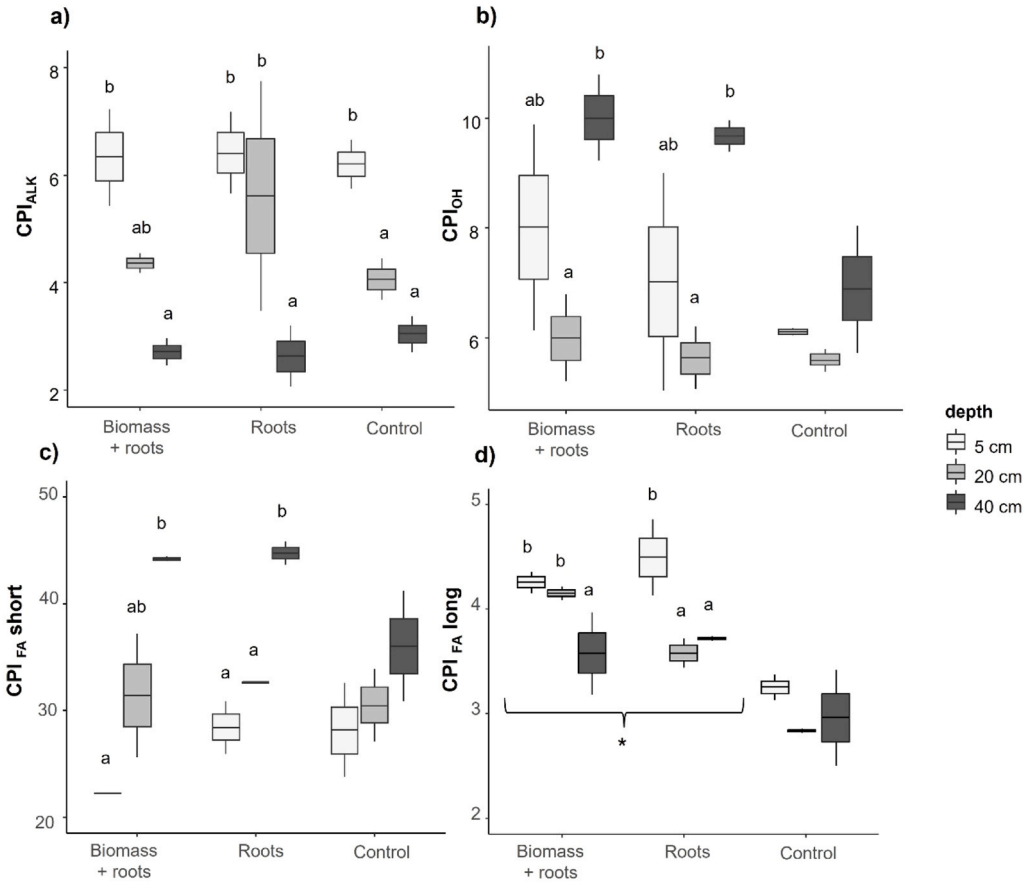

Fig. 4. Carbon preference index (CPI) for a) n-alkanes, b) n-alkanols, c) short-chain (C_{12}-C_{22}) and d) mid-, long-chain (C_{23}-C_{32}) n-fatty acids. Values are expressed as mean ± SE (n = 4). Significant effects between depth are indicated with lowercase letters ($p < 0.05$; Tukey HSD); "*" denotes significant differences between treatments.

derived inputs.

Saturated fatty acids (C_{20}–C_{23}) ranged from –26.6 ± 0.7 to –32.2 ± 0.6 ‰ and were consistently enriched in both treatments, although enrichment was greatest at 0–5 cm under treatment A (Fig. 9a), reflecting rapid microbial assimilation of aboveground residues. The unsaturated C_{22}:1 FA showed pronounced enrichment in the upper 20 cm, especially in biomass+root plots. Hydroxy acids showed the clearest differentiation between treatments. α-C_{20}-OH was significantly enriched across the profile in treatment B, while α-C_{24}-OH was enriched at 40 cm ($p < 0.01$). Conversely, α-C_{16}-OH was more enriched in surface soils under treatment A. ω-hydroxy acids were also enriched in treatments, with ω-C_{16} showing a strong surface signal under root-only conditions.

Branched fatty acids (iso- and anteiso-$C_{15:0}$, $C_{17:0}$) were enriched in both treatments but showed an additional depth-related enrichment in treatment B. Sterols showed $\delta^{13}C$ values between –18.7 ± 0.3 and –35.0 ± 0.2 ‰. Significant enrichment occurred primarily in the surface 0–5 cm for total sterols ($p < 0.05$), while stigmasterol was enriched down to 20 cm in both treatments, suggesting incorporation of maize phytosterols beyond the surface layer (Fig. 9b).

3.4. Estimation of C turnover

Based on bulk soil $\delta^{13}C$ values and compound-specific isotope analyses, we estimated the proportion of maize-derived C and turnover times across treatments and depths (Fig. 10). Treatments A (biomass+root) and B (root-only) added between 2.4 % and 13.9 % new C to soil organic matter, with significantly higher inputs in the surface layer of treatment A (Fig. 10a). Across depths, maize-derived C was incorporated into bulk SOM and all lipid classes, with contributions reaching up to 40 %. Bulk SOM showed the lowest proportional enrichment, while unsaturated fatty acids contributed the least among specific compounds. Hydroxy acids, long-chain *n*-alkanes, and sterols displayed the highest proportions of maize-derived C, with significant treatment effects in several depths, especially for sterols and *n*-alkanes ($p < 0.05$).

Turnover times (MRT) increased with depth for bulk SOM, and several compound classes showed significant treatment differences (Fig. 10b). On the surface, bulk SOC had significantly longer MRTs in treatment B compared to treatment A (27.8 ± 2.7 vs 15.2 ± 2.3 days; $p < 0.05$). At 20 cm, the trend was reversed, with significantly longer MRTs in treatment A showing longer MRTs (30.4 ± 3.7 days) relative to treatment B (16.7 ± 4.1 days; $p < 0.05$). At 40 cm, *n*-alkanes exhibited the longest MRTs among lipid classes, and sterols and hydroxy acids also showed significant contrasts between treatments. Across compound classes, FAs, unsaturated FAs, and *n*-alkanes showed shorter MRTs in treatment A at the surface, but treatment differences were less pronounced with depth.

4. Discussion

Bulk parameters provided important context for interpreting biomarker and isotopic patterns. $\delta^{13}C$ values were consistently more depleted in control plots than in treatments, reflecting incorporation of maize-derived carbon into bulk soil even in the absence of measurable SOC gains. As expected, SOC contents declined with depth, yet by contrast no significant differences were observed between treatments. This finding allowed to assume steady-state conditions for assessing the

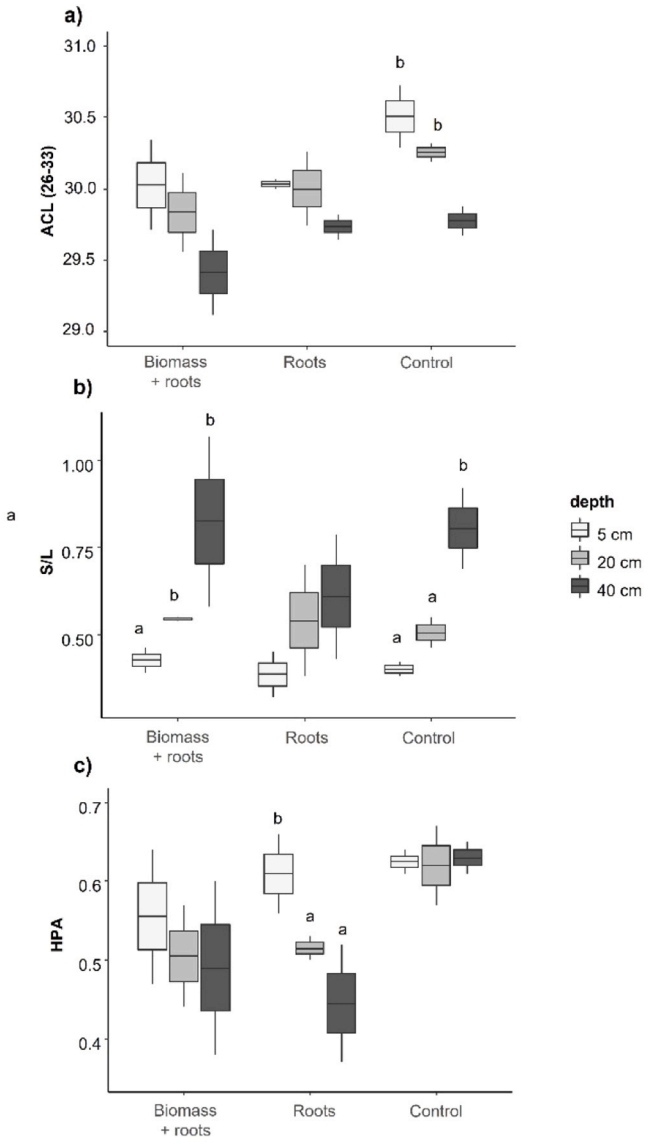

Fig. 5. Calculated indexes: a) average chain length (ACL) of n-alkanes; b) short-to-long chain n-alkanes index (S/L(15–26/27–32)); c) and Higher Plant Alkane (HPA) ratio. Values are expressed as mean ± SE (n = 3). Significant effects between depth are indicated with lowercase letters ($p < 0.05$, Tukey HSD).

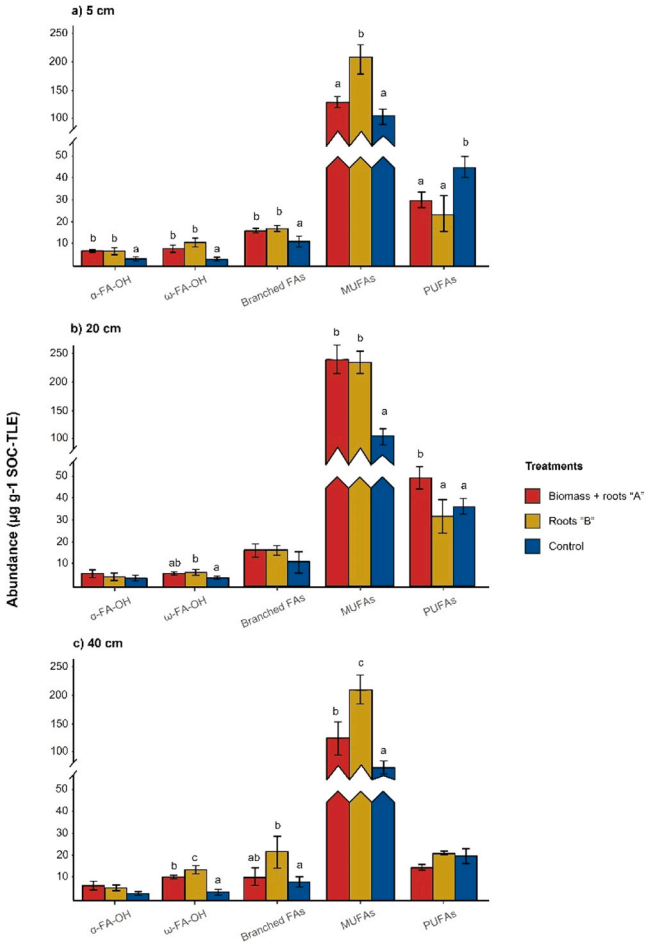

Fig. 6. Total abundances of α-, ω- hydroxy acids; branched and unsaturated (mono- and poly-) fatty acids across soil depths in the three treatments (mean ± SE, n = 4). Significant effects between treatments are indicated with lowercase letters ($p < 0.05$, Tukey HSD).

turnover of SOC (Amelung et al., 2008). Nevertheless, although the lack of significant changes in bulk SOC supports the use of a steady-state assumption for MRT calculations, it is important to acknowledge that the introduction of fresh maize-derived C may have induced short-term non–steady-state conditions, including potential priming effects. On one hand, this highlights the limited short-term impact of residue management on total SOC pools in Mediterranean soils, where rapid mineralization constrains C accumulation despite fresh inputs (Li et al., 2020; Angers et al., 2022). On the other hand, this indicates that immediate changes using ^{13}C-incubation approaches could better assess these potential non–steady-state conditions, allowing quantification of short-term CO_2 release, priming responses, and microbial uptake dynamics that cannot be resolved through end-point $\delta^{13}C$ measurements alone. Taken together, these patterns suggest that much of the maize-derived carbon incorporated during the 21-month period likely replaced mineralized native SOC rather than increasing total stocks, consistent with short-term priming and steady-state dynamics previously tested in this experimental trial (San-Emeterio et al., 2023b). Distinguishing between true accrual and replacement will require long-term monitoring combined with isotopic flux measurements to track whether newly incorporated carbon is ultimately stabilized or respired.

The relative proportion of extractable lipids (TLEs) to SOC did not differ significantly among treatments, indicating that fresh maize residues were rapidly transformed into microbial products rather than accumulated as extractable compounds. The decline of TLEs with depth mirrors the greater degradability of lipid fractions compared with bulk SOC, consistent with their preferential loss during decomposition (Holtvoeth et al., 2010). Taken together, these bulk parameters underline that while total SOC stocks remain stable over short timescales, isotopic and biomarker analyses reveal active processing of fresh maize-derived carbon within soil organic matter pools.

4.1. Lipid profile

4.1.1. n-alkanes

The dominance of C_{29} and C_{31} homologues confirms that the *n*-alkanes largely reflect plant wax inputs, as expected for maize residues, which produce odd-numbered long-chain homologues (Eglinton and Hamilton, 1967). The consistently lower abundances in the control plots suggest stronger SOC degradation in the absence of fresh maize-derived material, consistent with earlier observations in Mediterranean soils where organic matter is highly mineralized (Routh et al., 2014).

The CPI_{ALK} values above 2 indicate relatively good preservation of hydrocarbons (Andersson and Meyers, 2012). Their increase at 20 cm in

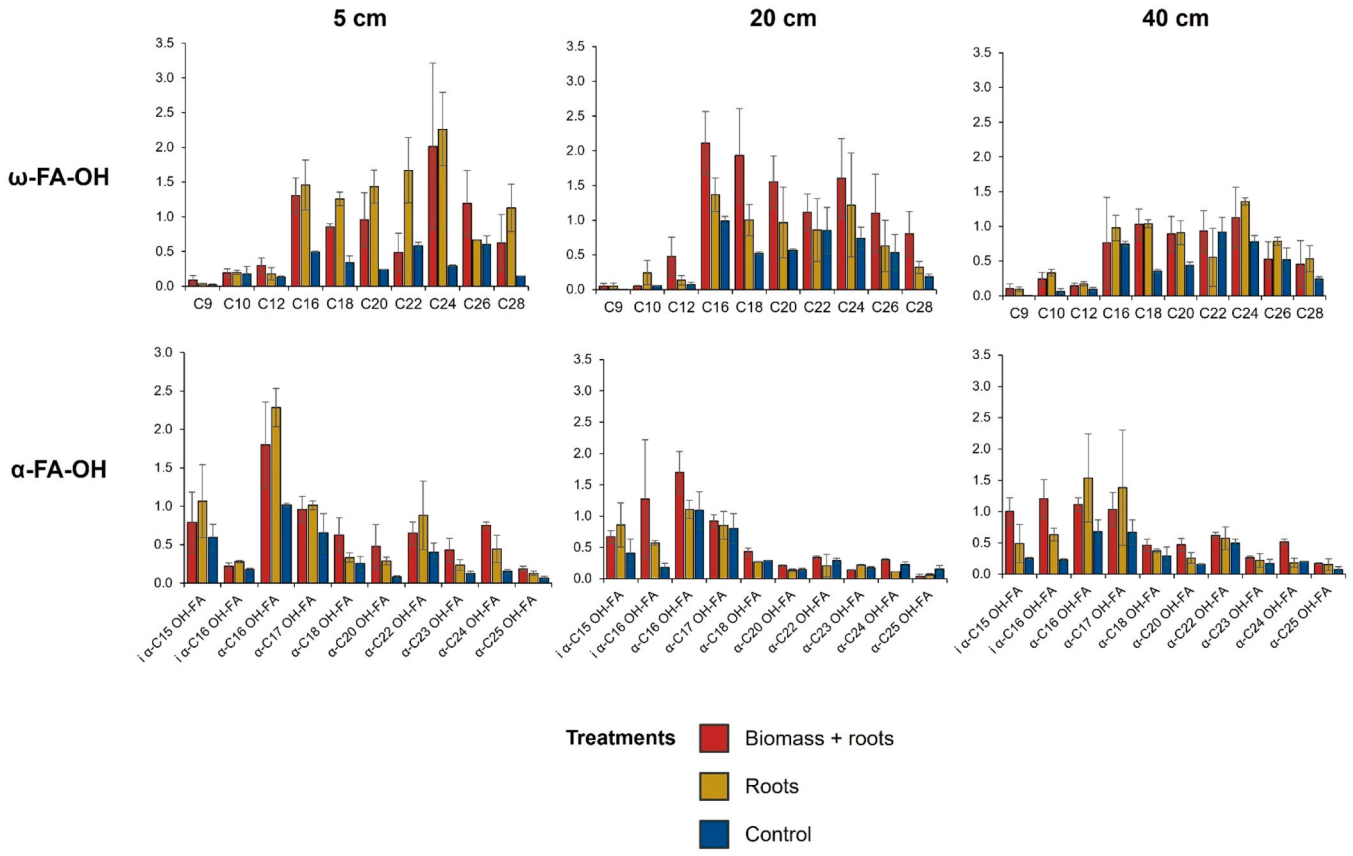

Fig. 7. Distribution of ω-hydroxy (ω-FA-OH) and α-hydroxy (α-FA-OH) acids across soil depths in all treatments. Values represent mean ± SE (n = 4).

the root-only treatment suggests that deeper *n*-alkane signals were maintained by root-derived inputs and microbial recycling, in line with studies emphasizing the role of roots in supplying more stable carbon fractions at depth (Angst et al., 2016). Similarly, ACL values near 30 are typical of higher plant waxes, while their decline at 40 cm may indicate a stronger influence of microbial short-chain homologues (González-Vila et al., 2003).

The S/L ratio patterns further support this interpretation. A lower ratio in the surface soils of biomass+root plots indicates the predominance of long-chain homologues from maize residues, whereas the higher values at depth reflect increased contributions of short-chain compounds from microbial sources (Wiesenberg et al., 2009). The lack of a depth effect in treatment B suggests that root-derived inputs maintained the plant wax signal deeper in the soil. Finally, the decline of the HPA index with depth under treatment B points to enhanced decomposition of alkanols relative to alkanes in the rhizosphere, consistent with aerobic microbial activity around maize roots (Poynter and Eglinton, 1990; Routh et al., 2014).

4.1.2. *n*-alkanols

The strong even-over-odd predominance of *n*-alkanols complements the odd-over-even signal of *n*-alkanes, together confirming that the lipid inputs are primarily plant-derived (Rielley et al., 1991; Van Bergen et al., 1997). The bimodal distribution, with peaks at both short- and long-chain homologues, reflects contributions from microbial lipids (C_{18}) and higher plant waxes ($C_{28–30}$) (Otto et al., 2005; Li et al., 2015; 2022).

The significant enrichment of short- and mid-chain homologues in the biomass+root treatment at the soil surface suggests enhanced microbial activity fueled by aboveground maize residues. This contrasts with the root-only treatment, where intermediate values point to more modest stimulation. The absence of differences below 5 cm indicates that alkanols from surface residues were not translocated downward, emphasizing the localized impact of surface litter inputs.

The depth-related increase in CPI_{OH} in treatment plots, particularly at 40 cm, suggests the accumulation of secondary alkanol products during SOM degradation (Simoneit and Mazurek, 2007; Zheng et al., 2007). The lack of a similar trend in controls highlights the role of maize-derived inputs in shaping this pattern. Moreover, the inverse relationship between CPI_{OH} and CPI_{ALK} points to differential preservation pathways for alkanes and alkanols: while alkanes are relatively resistant, alkanols may undergo more extensive microbial reworking (Thomas et al., 2021). Lower CPI_{OH} values (< 6) in surface soils under treatments likely reflect this enhanced microbial processing, stimulated by the fresh maize inputs.

4.1.3. *n*-alkanoic acids

The dominance of C_{16} reflects strong microbial contributions, consistent with its role as a key membrane lipid (Eglinton and Hamilton, 1967). The enrichment of short-chain homologues in the topsoil under both maize treatments indicates enhanced microbial activity fueled by fresh C inputs, in agreement with previous studies showing bacterial preference for C_{16} and C_{18} fatty acids (Nierop et al., 2005).

By contrast, the persistence of long-chain homologues points to inputs from maize leaf waxes, while C_{22} and C_{24} likely reflect a combination of wax- and root-derived suberin contributions. The depth trend in CPI values supports this interpretation: lower $CPI_{FA\text{-}short}$ values at the surface indicate stronger microbial reworking of fatty acids where residue-derived C is most available, whereas higher values at depth reflect reduced alteration. Conversely, the higher $CPI_{FA\text{-}long}$ values in treatment plots suggest reduced degradation of plant-derived long-chain FAs (Ren et al., 2016), highlighting their relative stability in comparison with the more labile short-chain homologues. Together, these patterns suggest that maize inputs stimulate microbial activity near the surface,

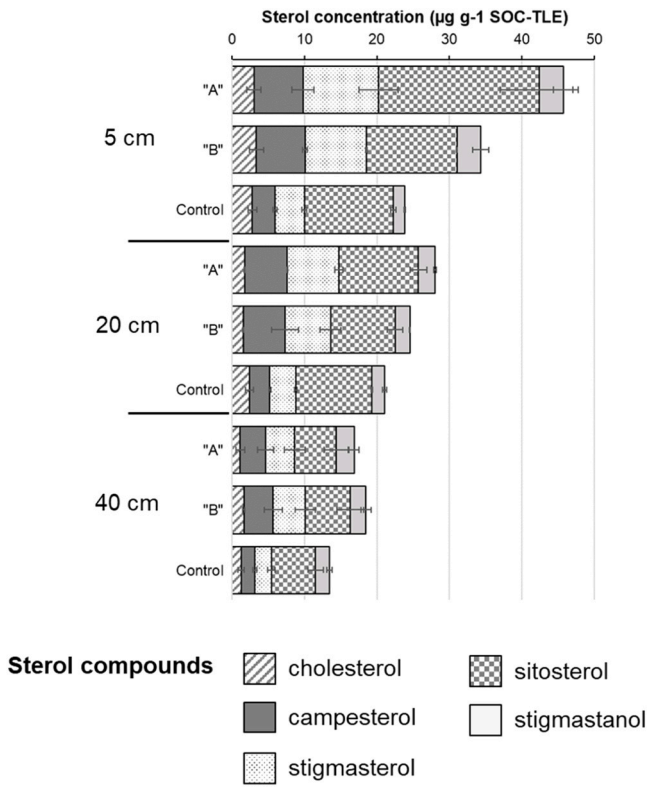

Fig. 8. Vertical distribution of major sterols across soil depths (0–5, 5–20, and 20–40 cm) under the three treatments. Abundances of cholesterol (C_{27}), campesterol (C_{28}), stigmasterol (C_{29}), sitosterol (C_{29}), and stigmastanol (C_{29}) are shown as mean ± SE (n = 4).

while root-derived lipids contribute more persistently to deeper layers.

As for the mono- and polyunsaturated FAs, the high relative abundances of $C_{16:1}$ and $C_{18:1}$ homologues indicate active microbial processing, since these unsaturated fatty acids are widely synthesized by bacteria and plants but are highly labile (Bobbie and White, 1980; Zelles and Bai, 1993). Their predominance in surface soils under maize treatments reflects stimulation of microbial communities by fresh inputs of labile C. The particularly strong signal of $C_{16:1cis9}$ and $C_{18:1}$ homologues in biomass+root plots suggests that aboveground residues provided additional substrates that accelerated microbial lipid synthesis. In contrast, the enrichment of $C_{22:1}$ isomers at 40 cm in root-only plots points to a distinct pathway: unsaturated lipids associated with root tissues or root exudates that are incorporated deeper in the soil (Chávez-Lara et al., 2019). These depth-specific differences illustrate how above- and belowground inputs differentially shape microbial activity and lipid turnover in the soil profile.

Branched FAs are reliable markers of bacterial inputs, especially Actinomycetes and Gram-positive bacteria (Zelles, 1999; Quezada et al., 2007). Their increased abundance in the maize treatments demonstrates the stimulation of microbial biomass by fresh plant-derived inputs. The strong signal at depth in the root-only treatment highlights the importance of rhizodeposition and root turnover in sustaining microbial activity in subsoils. This finding reinforces the idea that root-derived C, though less abundant than surface litter, may disproportionately fuel microbial processes and contribute to deeper incorporation of new C into soil organic matter (Ludwig et al., 2015).

Lastly, the bimodal distributions of both ω- and α-hydroxy acids are consistent with contributions from plant biopolyesters. ω-hydroxy acids, particularly ω-C_{16}, derive from both cutin (leaves) and suberin (roots), whereas ω-C_{22} and ω-C_{24} are mainly associated with suberin in root tissues (Bull et al., 2000; Kolattukudy, 2001; Nierop et al., 2005). The strong presence of these mid- and long-chain ω-hydroxy acids at depth in the treatment plots, especially in root-only soils, points to root-derived suberin as a key contributor to deep soil carbon inputs.

In contrast, the relative enrichment of α-hydroxy acids in surface soils under the biomass+root treatment highlights microbial activity. Compounds such as α-C_{18} and short-chain α-$C_{15–16}$ are well-established markers of Gram-negative bacteria (Langer and Rinklebe, 2009; Holtvoeth et al., 2010), suggesting that aboveground maize residues stimulated microbial processing in the upper soil.

These results altogether showed that, even in shallow-rooted crops such as maize, above- and belowground inputs follow fundamentally different pathways of incorporation into SOM. Aboveground residues

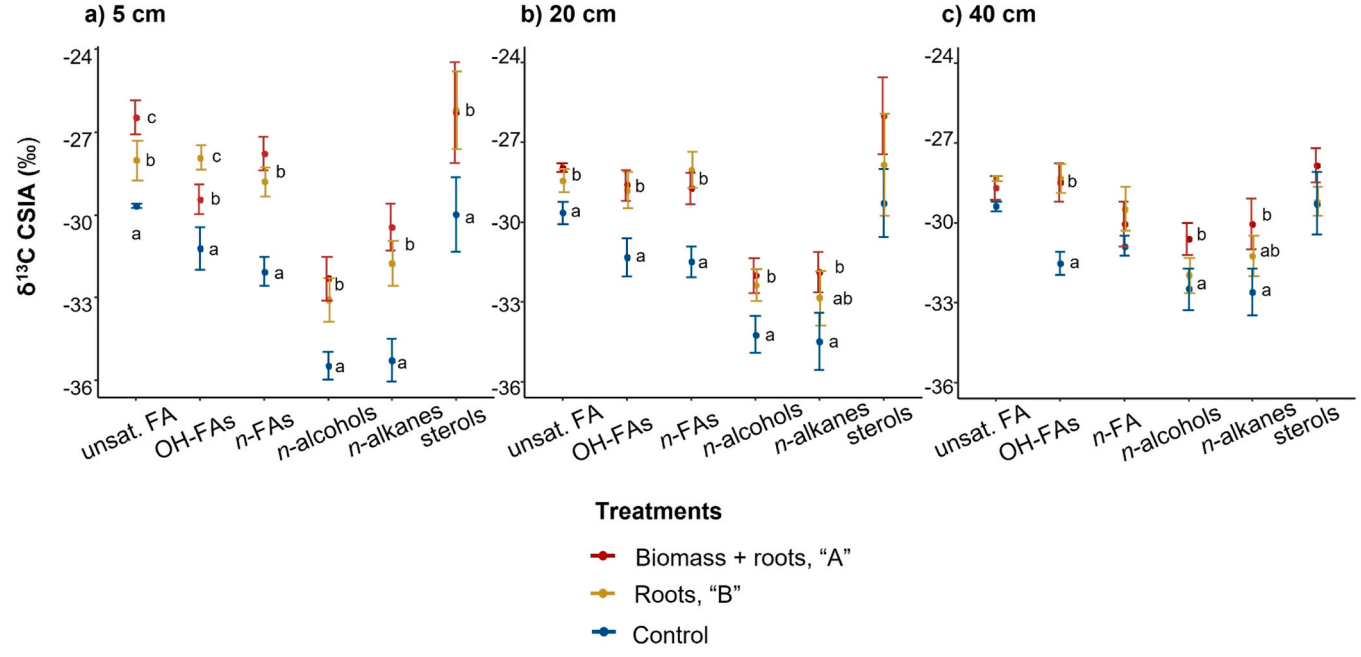

Fig. 9. Average $\delta^{13}C$ ranges (mean ± SE, n = 4) of the diverse compounds identified by CSIA between treatments for each depth: a) 5 cm, b) 20 cm, c) 40 cm. Letters indicate significant differences between treatments for each group of compounds ($p < 0.05$, Dunn Test).

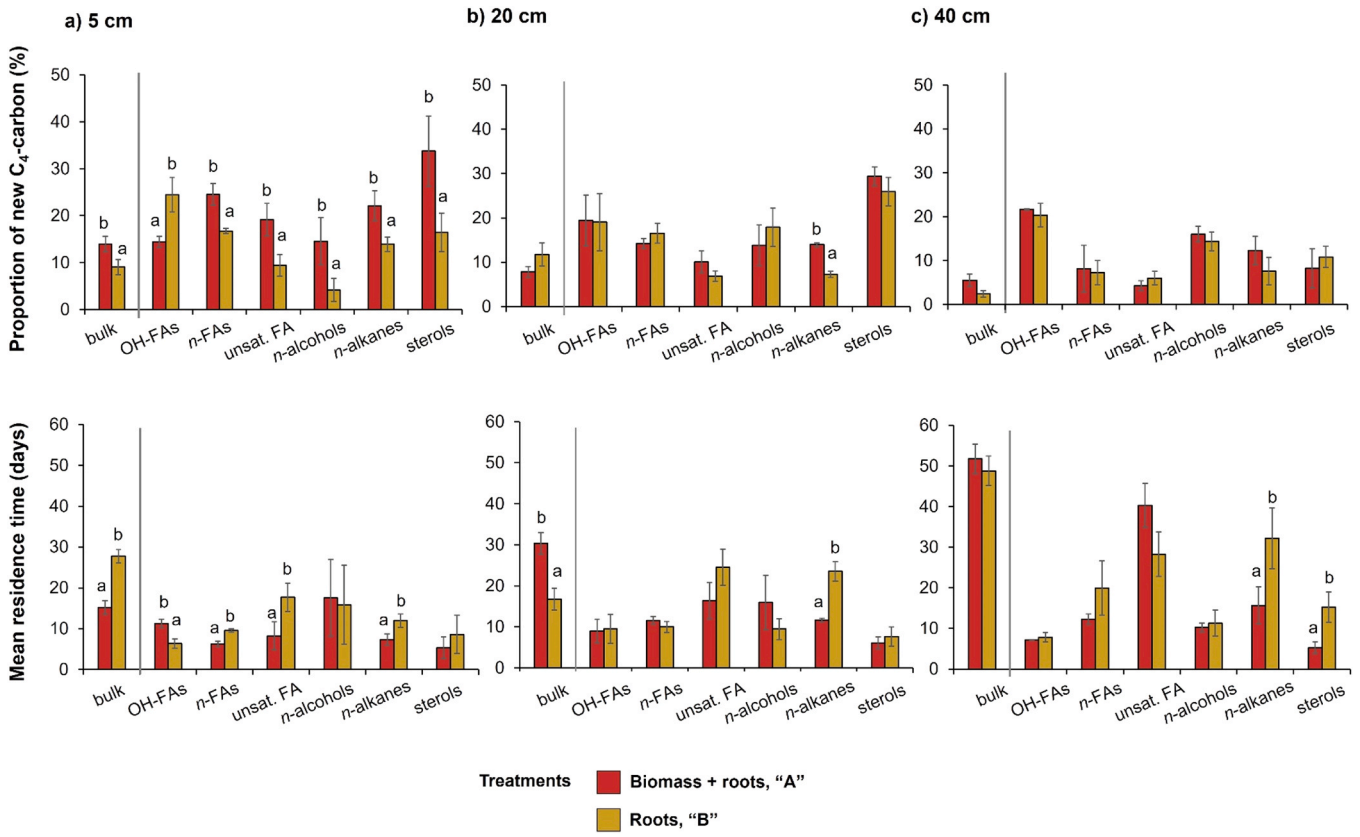

Fig. 10. Calculation of a) proportion of new C_4-derived carbon (%) according to the two different treatments, and b) turnover time calculations, expressed in mean residence time (MRT, days) based on new C_4-C proportions. Both parameters are reported for bulk SOC and average of the different groups of lipids. Values are reported as average (n = 4 ± SE).

accumulate at the surface, where they undergo rapid microbial decomposition, leading to short-lived increases in microbial-derived carbon and surface SOC. In contrast, maize roots introduce carbon directly into deeper soil layers through rhizodeposition, fine-root turnover, and the decay of suberin-rich tissues. These compounds enter subsoil horizons in situ, bypassing the highly oxidative surface environment. Taken together, these patterns indicate that aboveground residues enhanced microbial contributions in surface soils, whereas roots supplied more resistant suberin-derived compounds to deeper horizons. This duality underscores the contrasting roles of plant compartments in shaping the vertical distribution and turnover of hydroxy acids in SOM.

4.1.4. Sterols

The detection of C_{28} and C_{29} sterols reflects contributions from higher plant waxes, while cholesterol likely derives from fungi and soil fauna (Rielley et al., 1991; Pancost et al., 2002; Puglisi et al., 2003). The elevated concentrations of campesterol and stigmasterol in the maize treatments confirm the incorporation of aboveground plant inputs, particularly in surface soils where residues were deposited.

Sterols are often considered relatively stable biomarkers compared to other lipids, as they lack easily degradable functional groups (Van Bergen et al., 1997). However, their strong decline with depth in all plots indicates that they are also subject to decomposition and microbial assimilation. The consistently lower concentrations in control soils suggest accelerated SOM mineralization when fresh inputs are absent, leading to sterol loss through degradation (Heumann et al., 2011; Vanmierlo et al., 2013).

Overall, sterols reinforce the broader pattern observed across other lipid classes: the biomass+root treatment promotes greater inputs and preservation of plant-derived compounds at the surface, whereas the absence of residues in the control leads to stronger microbial consumption and depletion.

4.2. Compound specific stable carbon isotope composition of lipids ($\delta^{13}C$ CSIA)

The $\delta^{13}C$ patterns across compound classes highlight both the distinct biosynthetic origins of lipids and their contrasting roles in carbon cycling. Both *n*-alkanes and *n*-alkanols were consistently more depleted than other compound groups, in agreement with the general depletion of leaf wax-derived alkanes compared to root- or microbially derived compounds (Wiesenberg et al., 2004). Their enrichment in treatment plots confirms maize inputs, with the strongest signal in surface soils where aboveground residues were added. Interestingly, enrichment of long-chain alkanes at depth in control soils suggests contributions from older C_3 vegetation stabilized in SOM (Rumpel et al., 2004; Crow et al., 2009; Wu et al., 2019).

Fatty acids showed stronger enrichment than alkanes, particularly in the short- and mid-chain homologues, indicating their dynamic role in microbial processing. The enhanced enrichment in topsoil of treatment A supports the idea that fresh aboveground residues stimulate microbial uptake of maize-derived C. Similar enrichment of unsaturated $C_{22:1}$ FA in biomass+root plots points to its rapid turnover and preferential use of maize C by microbial communities (Kindler et al., 2009; Knief et al., 2020).

Hydroxy acids clearly differentiate between the above- and belowground inputs. Enrichment of α-C_{20}-OH in root-only plots reflects microbial reworking of root exudates (Hobbie and Werner, 2004; Bull et al., 2000; Angst et al., 2016). Deeper enrichment of α-C_{24}-OH highlights suberin contributions from roots (Kolattukudy, 2001; Feng et al., 2010), while surface enrichment of α-C_{16}-OH in biomass+root plots

reflects microbial activity stimulated by residue addition. The contrasting behaviors of α- and ω-hydroxy acids can be attributed to their degradation pathways: ω-hydroxy acids, more closely linked to suberin, are relatively resistant to decomposition, whereas α-hydroxy acids are more strongly associated with microbial activity and thus more dynamic (Mendez-Millan et al., 2011).

Microbial markers further confirm these trends. Branched fatty acids were strongly enriched in both treatments, especially in surface soils, indicating active microbial assimilation of maize C (Zelles, 1999; Quezada et al., 2007). Their additional enrichment at depth in treatment B underscores the role of rhizodeposition in stimulating bacterial activity and incorporation of root-derived C.

Sterols, though generally less responsive, showed enrichment in surface soils under both treatments. Enrichment of stigmasterol down to 20 cm indicates that phytosterols from maize were incorporated beyond the immediate surface, though their relatively labile nature may explain weaker signals compared to hydroxy acids and fatty acids (Bull et al., 2000; Heumann et al., 2011).

The consistent enrichment of compound-specific lipids compared to bulk SOM confirms that CSIA provides a more sensitive measure of new C incorporation (Paterson et al., 2007). Bulk $\delta^{13}C$ values average across pools and processes, obscuring the dynamics captured at the biomarker level.

Overall, $\delta^{13}C$-CSIA reveals complementary pathways of maize-derived C incorporation. Aboveground residues (treatment A) enhanced enrichment in surface plant waxes and microbial lipids, reflecting rapid cycling and microbial assimilation. Root-only inputs (treatment B) disproportionately enriched suberin-derived hydroxy acids and bacterial markers at depth, indicating that roots contributes to pools with a longer mean residence time, potentially acting as a more persistent pathway for incorporating this new, C_4-derived carbon into subsoils. These compound-specific isotopic shifts corroborate the concentration data and highlight how residue management mediates both the depth distribution and the fate of new C inputs in Mediterranean cropping systems.

Taken together, the $\delta^{13}C$-CSIA results demonstrate complementary roles of above- and belowground inputs in shaping the isotopic composition of soil lipids. Aboveground residues mainly influenced surface lipids, including plant wax *n*-alkanes and microbial-derived unsaturated FAs, while root inputs contributed to the isotopic enrichment of suberin-derived hydroxy acids and bacterial lipids at depth. These findings corroborate the concentration data and support our hypothesis that aboveground inputs stimulate microbial incorporation of maize-derived C near the surface, whereas belowground, root-related inputs showed a higher potential for a higher persistence of carbon in deeper soil horizons.

4.3. Estimation of C turnover

The isotopic mass-balance approach revealed that both maize treatments contributed new carbon to SOM throughout the soil profile, but the pathways differed between above- and belowground inputs. The greater enrichment in the biomass+root treatment at the surface reflects the rapid incorporation of aboveground maize residues, which enhanced microbial assimilation but also led to faster turnover, as indicated by shorter MRTs. This pattern aligns with recent findings that aboveground residue inputs can increase microbial carbon use efficiency but simultaneously accelerate priming and turnover of SOM (Xie et al., 2022), and that incorporation of maize residues promotes rapid accumulation of particulate organic carbon fractions (Wang et al., 2020). In contrast, the root-only treatment showed slower C incorporation at the surface but longer MRTs, suggesting that the absence of surface litter limited labile inputs, leading to slower cycling of existing pools. Similar patterns have been observed in litter manipulation experiments, where exclusion of aboveground residues reduced short-term C turnover while root inputs promoted the formation of more stable SOM (Lajtha et al., 2014; Zeng et al., 2024).

At 20 cm, the reversal in MRT patterns —with longer residence times in treatment A— suggests that degradation products from maize residues were transferred down the profile and contributed to SOM pools with a higher potential for persistance. This agrees with previous studies showing that decomposition of aboveground biomass can generate soluble by-products that percolate into subsoils and stabilize (Crow et al., 2009). At 40 cm, the particularly long MRTs of *n*-alkanes are consistent with their recalcitrance, due to the absence of functional groups that make them resistant to microbial attack (Lichtfouse et al., 1998). This stability is well documented, as *n*-alkanes undergo limited transformation from plant to soil (Thomas et al., 2021), and their isotopic composition often reflects inherited vegetation signals due to their persistence in soils (Rao et al., 2017).

Compound-specific differences also align with their biochemical reactivity. Unsaturated fatty acids, which contain double bonds prone to microbial and abiotic degradation, incorporated maize-derived C rapidly but cycled out within the 21-month period, explaining their low contributions (Nierop et al., 2003). In contrast, hydroxy acids and sterols accumulated larger proportions of maize-derived C, reflecting their relative stability and association with suberin and structural plant components. This greater persistence of hydroxy acids arises from their biochemical structure: ω-hydroxy and mid-chain hydroxy acids are integral constituents of suberin, a highly aliphatic and cross-linked polyester that decomposes slowly and can strongly associate with mineral surfaces via polar functional groups (Yang et al., 2020). By contrast, unsaturated fatty acids contain double bonds and shorter chains that are more chemically reactive and readily accessible to enzymatic attack, which accelerates their decay and shortens their residence time (Zelles, 1999; Yang et al., 2020). Additionally, root-derived suberin compounds have previously been shown to contribute significantly to SOC profiles (Mendez-Millan et al., 2012), while sterols, despite being more labile than alkanes, can also persist in arable soils and thus provide useful indicators of plant inputs (Wiesenberg, 2004).

In addition to microbial processing, abiotic stabilization mechanisms could potentially contribute to the depth-specific MRT patterns observed. Small, labile compounds such as short-chain fatty acids, unsaturated FAs, and low–molecular weight alkanes can be rapidly sorbed onto reactive mineral surfaces —including Fe/Al (oxyhydr)oxides and clay minerals— which can slow decomposition and increase their apparent residence times at depth (Van Hees et al., 2003; Kleber et al., 2015). Moreover, subsoils experience fluctuating redox microsites that facilitate oxidative reactions driven by hydroxyl radicals (·OH) and Fenton-type chemistry, accelerating transformation of unsaturated and functionalized lipids and increasing thus C mineralization (Chen et al., 2020; Yu and Kuzyakov, 2021). These abiotic pathways provide complementary explanations for why MRTs of small-molecule lipids did not decrease uniformly with depth and why treatment differences were attenuated in deeper horizons.

Because suberin-associated lipids and microbially processed rhizodeposits have slower turnover rates and form stronger associations with minerals, they contribute more persistently to SOC stabilization at depth. This mechanistic distinction explains why shallow-rooted crops can still generate deeper and longer-lived carbon inputs compared with surface residues. Nevertheless, it is appropriate to recall to the above-mentioned mineral interactions as for a potential cause for this C stabilization, as suberin-derived lipids are known to bind efficiently to reactive mineral phases (Spielvogel et al., 2014). This may complement the explanation of more enduring carbon pools observed in the root-only treatment.

Overall, these results highlight a dual dynamic: aboveground residues drive rapid but short-lived incorporation of maize-derived carbon into labile microbial and FA pools, whereas root-derived inputs and residue-derived by-products contribute to longer-lived SOM fractions in deeper horizons This partitioning into “fast” and “slow” pools underscores the importance of residue management in determining not

only the amount but also the persistence of new C in agricultural soils. Nevertheless, these results taken together should be interpreted as evidence of short-term biochemical retention and early routing of new carbon into specific molecular pools, rather than confirmation of long-term SOC sequestration.

5. Conclusions

This study provides new insights into soil organic carbon (SOC) dynamics in Mediterranean agricultural soils, where low organic matter content and high mineralization rates limit carbon stabilization. By combining lipid biomarker analysis with compound-specific stable isotope analysis (CSIA), we traced the incorporation of C_4-derived carbon following a crop shift from wheat to maize. Even within 21 months, significant maize-derived C was incorporated into SOM, both through direct residue inputs and microbial assimilation.

Our results show that long-chain *n*-alkanes (C_{29}, C_{31}) served as robust indicators of direct aboveground plant residue inputs, whereas fatty acids and hydroxy acids revealed complementary signals of microbial reworking and root-derived carbon at depth. Isotopic enrichment patterns highlighted rapid cycling of labile fractions in surface soils, contrasted with the greater short-term retention of root- and suberin-derived lipids in deeper horizons. These compound-specific signals were more sensitive than bulk $\delta^{13}C$ measurements, which tended to mask short-term dynamics.

Overall, our findings underline the dual role of biomass and roots in shaping SOM composition and turnover: aboveground inputs drive fast but transient microbial cycling, while roots contribute to carbon inputs that are retained longer in subsoils over the study period. This duality emphasizes both the challenges and opportunities of enhancing carbon sequestration in Mediterranean soils. Future studies should explicitly quantify mineral-associated organic matter fractions and mineral–organic interactions to determine whether the short-term biochemical pathways identified here ultimately translate into long-term SOC stabilization in Mediterranean soils.

CRediT authorship contribution statement

Ian D. Bull: Writing – review & editing, Visualization, Validation, Supervision, Resources, Methodology, Investigation, Formal analysis, Data curation, Conceptualization. **Layla M. San-Emeterio:** Writing – review & editing, Writing – original draft, Visualization, Validation, Methodology, Investigation, Formal analysis, Data curation, Conceptualization. **Rafael López-Núñez:** Writing – review & editing, Validation, Supervision, Investigation. **Jens Holtvoeth:** Writing – review & editing, Validation, Supervision, Methodology, Investigation, Formal analysis, Data curation, Conceptualization. **José A. González-Pérez:** Writing – review & editing, Visualization, Validation, Supervision, Resources, Methodology, Investigation, Funding acquisition, Formal analysis, Data curation, Conceptualization.

Declaration of Competing Interest

The authors declare that they have no known competing financial interests or personal relationships that could have appeared to influence the work reported in this paper.

Acknowledgements

L.M. San Emeterio thanks Ministerio de Ciencia Innovación y Universidades (MICIU) for INTERCARBON project (CGL2016–78937-R). L. San Emeterio also thanks MICIU for funding FPI research grants (BES-2017–07968). D. Monis and A.M. Carmona are acknowledged for technical assistance.

Appendix A. Supporting information

Supplementary data associated with this article can be found in the online version at doi:10.1016/j.agee.2025.110179.

Data availability

Data will be made available on request.

References

Amelung, W., Brodowski, S., Sandhage-Hofmann, A., Bol, R., 2008. Combining biomarker with stable isotope analyses for assessing the transformation and turnover of soil organic matter. Adv. Agron. 100, 155–250. https://doi.org/10.1016/S0065-2113(08)00606-8.

Andersson, R.A., Meyers, P.A., 2012. Effect of climate change on delivery and degradation of lipid biomarkers in a Holocene peat sequence in the Eastern European Russian Arctic. Org. Geochem 53, 63–72. https://doi.org/10.1016/j.orggeochem.2012.05.002.

Andersson, R.A., Kuhry, P., Meyers, P., Zebühr, Y., Crill, P., Mörth, M., 2011. Impacts of paleohydrological changes on n-alkane biomarker compositions of a Holocene peat sequence in the eastern European Russian Arctic. Org. Geochem 42 (9), 1065–1075. https://doi.org/10.1016/j.orggeochem.2011.06.020.

Angers, D., Arrouays, D., Cardinael, R., Chenu, C., Corbeels, M., Demenois, J., Farrell, M.-, Martin, M., Minasny, B., Recous, S., Six, J., 2022. A well-established fact: Rapid mineralization of organic inputs is an important factor for soil carbon sequestration. Eur. J. Soil Sci. 73 (3), e13242. https://doi.org/10.1111/ejss.13242.

Angst, G., John, S., Mueller, C.W., Kögel-Knabner, I., Rethemeyer, J., 2016. Tracing the sources and spatial distribution of organic carbon in subsoils using a multi-biomarker approach. Sci. Rep. 6, 29478. https://doi.org/10.1038/srep29478.

Angst, G., Messinger, J., Greiner, M., Häusler, W., Hertel, D., Kirfel, K., Kögel-Knabner, I., Leuschner, C., Rethemeyer, J., Mueller, C.W., 2018. Soil organic carbon stocks in topsoil and subsoil controlled by parent material, carbon input in the rhizosphere, and microbial-derived compounds. Soil Biol. Biochem 122, 19–30. https://doi.org/10.1016/j.soilbio.2018.03.026.

Balesdent, J., Mariotti, A., 1996. Measurement of soil organic matter turnover using 13C natural abundance. In: Boutton, T.W., Yamasaki, S.I. (Eds.), Mass spectrometry of soils, pp. 83–111.

Balesdent, J., Mariotti, A., Guillet, B., 1987. Natural 13C abundance as a tracer for studies of soil organic matter dynamics. Soil Biol. Biochem 19 (1), 25–30. https://doi.org/10.1016/0038-0717(87)90120-9.

Bobbie, R.J., White, D.C., 1980. Characterization of benthic microbial community structure by high-resolution gas chromatography of fatty acid methyl esters. Appl. Environ. Microbiol 39 (6), 1212–1222. https://doi.org/10.1128/aem.39.6.1212-1222.1980.

Bull, I.D., van, Bergen, P.F., Nott, C.J., Poulton, P.R., Evershed, R.P., 2000. Organic geochemical studies of soils from the Rothamsted classical experiments—V. The fate of lipids in different long-term experiments. Org. Geochem 31 (5), 389–408. https://doi.org/10.1016/S0146-6380(00)00008-5.

Bush, R.T., McInerney, F.A., 2013. Leaf wax n-alkane distributions in and across modern plants: implications for paleoecology and chemotaxonomy. Geochim. Cosmochim. Acta 117, 161–179. https://doi.org/10.1016/j.gca.2013.04.016.

Chávez-Lara, C.M., Holtvoeth, J., Roy, P.D., Pancost, R.D., 2019. Lipid biomarkers in lacustrine sediments of subtropical northeastern Mexico and inferred ecosystem changes during the late Pleistocene and Holocene. Palaeogeograp Palaeocli 535, 109343. https://doi.org/10.1016/j.palaeo.2019.109343.

Chen, C., Hall, S.J., Coward, E., Thompson, A., 2020. Iron-mediated organic matter decomposition in humid soils can counteract protection. Nat. Commun. 11 (1), 2255. https://doi.org/10.1038/s41467-020-16071-5.

Collins, H.P., Christenson, D.R., Blevins, R.L., Bundy, L.G., Dick, W.A., Huggins, D.R., Paul, E.A., 1999. Soil carbon dynamics in corn-based agroecosystems: Results from carbon-13 natural abundance. Soil Sci. Soc. Am. J. 63 (3), 584–591. https://doi.org/10.2136/sssaj1999.03615995006300030022x.

Coplen, T.B., 2011. Guidelines and recommended terms for expression of stable-isotope-ratio and gas-ratio measurement results. Rapid Commun. Mass Spectrom. 25 (17), 2538–2560. https://doi.org/10.1002/rcm.5129.

Cranwell, P.A., 1973. Chain-length distribution of n-alkanes from lake sediments in relation to post-glacial environmental change. Freshw. Biol. 3 (3), 259–265. https://doi.org/10.1111/j.1365-2427.1973.tb00921.x.

Crow, S.E., Lajtha, K., Filley, T.R., Swanston, C.W., Bowden, R.D., Caldwell, B.A., 2009. Sources of plant-derived carbon and stability of organic matter in soil: implications for global change. Glob. Change Biol. 15 (8), 2003–2019. https://doi.org/10.1111/j.1365-2486.2009.01850.x.

Eglinton, G., Hamilton, R.J., 1967. Leaf Epicuticular Waxes: The waxy outer surfaces of most plants display a wide diversity of fine structure and chemical constituents. Science 156 (3780), 1322–1335. https://doi.org/10.1126/science.156.3780.1322.

Fanin, N., Bertrand, I., 2016. Aboveground litter quality is a better predictor than belowground microbial communities when estimating carbon mineralization along a land-use gradient. Soil Biol. Biochem 94, 48–60. https://doi.org/10.1016/j.soilbio.2015.11.007.

Feng, X., Xu, Y., Jaffé, R., Schlesinger, W.H., Simpson, M.J., 2010. Turnover rates of hydrolysable aliphatic lipids in Duke Forest soils determined by compound specific

13C isotopic analysis. Org. Geochem 41 (6), 573–579. https://doi.org/10.1016/j.orggeochem.2010.02.013.
Ferreira, C.S.S., Keesstra, S., Destouni, G., Solomun, M.K., Kalantari, Z., 2024. Soil degradation in the Mediterranean region: drivers and future trends. Environmental Sustainability in the Mediterranean Region: Challenges and Solutions. Springer International Publishing, Cham, pp. 81–112. https://doi.org/10.1007/978-3-031-64503-7_5.
Francaviglia, R., Ledda, L., Farina, R., 2018. Organic carbon and ecosystem services in agricultural soils of the Mediterranean Basin. Sustainable Agriculture Reviews 28: Ecology for Agriculture. Springer International Publishing, Cham, pp. 183–210. https://doi.org/10.1007/978-3-319-90309-5_6.
Fu, H., Chen, H., Ma, Z., Liang, G., Chadwick, D.R., Jones, D.L., Wanek, W., Wu, L., Ma, Q., 2025. Fungal Necromass Carbon Dominates Global Soil Organic Carbon Storage. Glob. Change Biol. 31 (8), e70413. https://doi.org/10.1111/gcb.70413.
Gonzalez-Vila, F.J., Polvillo, O., Boski, T., Moura, D., de Andrés, J.R., 2003. Biomarker patterns in a time-resolved Holocene/terminal Pleistocene sedimentary sequence from the Guadiana river estuarine area (SW Portugal/Spain border). Org. Geochem 34 (12), 1601–1613. https://doi.org/10.1016/j.orggeochem.2003.08.006.
Heumann, S., Schlichting, A., Böttcher, J., Leinweber, P., 2011. Sterols in soil organic matter in relation to nitrogen mineralization in sandy arable soils. J. Plant Nutr. Soil Sci. 174 (4), 576–586. https://doi.org/10.1002/jpln.200900273.
Hirave, P., Wiesenberg, G.L., Birkholz, A., Alewell, C., 2020. Understanding the effects of early degradation on isotopic tracers: implications for sediment source attribution using compound-specific isotope analysis (CSIA). Biogeosciences 17 (8), 2169–2180. https://doi.org/10.5194/bg-17-2169-2020.
Hobbie, E.A., Werner, R.A., 2004. Intramolecular, compound-specific, and bulk carbon isotope patterns in C3 and C4 plants: a review and synthesis. N. Phytol. 161 (2), 371–385. https://doi.org/10.1111/j.1469-8137.2004.00970.x.
Holtvoeth, J., Vogel, H., Wagner, B., Wolff, G.A., 2010. Lipid biomarkers in Holocene and glacial sediments from ancient Lake Ohrid (Macedonia, Albania). Biogeosciences 7 (11), 3473–3489. https://doi.org/10.5194/bg-7-3473-2010.
Holtvoeth, J., Rushworth, D., Copsey, H., Imeri, A., Cara, M., Vogel, H., Wagner, T., Wolff, G.A., 2016. Improved end-member characterisation of modern organic matter pools in the Ohrid Basin (Albania, Macedonia) and evaluation of new palaeoenvironmental proxies. Biogeosciences 13 (3), 795–816. https://doi.org/10.5194/bg-13-795-2016.
IUSS Working Group WRB, 2014. World Reference Base for Soil Resources 2014. World Soil Resources Reports No. 106. Update 2015: International Soil Classification System for Naming Soils and Creating Legends for Soil Maps. FAO, Rome.
Kindler, R., Miltner, A., Thullner, M., Richnow, H.H., Kästner, M., 2009. Fate of bacterial biomass derived fatty acids in soil and their contribution to soil organic matter. Org. Geochem 40 (1), 29–37. https://doi.org/10.1016/j.orggeochem.2008.09.005.
Kleber, M., Eusterhues, K., Keiluweit, M., Mikutta, C., Mikutta, R., Nico, P.S., 2015. Chapter One - Mineral–organic associations: formation, properties, and relevance in soil environments. Adv. Agron. 130, 1–140. https://doi.org/10.1016/bs.agron.2014.10.005.
Knief, C., Bol, R., Amelung, W., Kusch, S., Frindte, K., Eckmeier, E., Jaeschke, A., Dunai, T., Fuentes, B., Mörchen, R., Schütte, T., Lücke, A., Klumpp, E., Kaiser, K., Rethemeyer, J., 2020. Tracing elevational changes in microbial life and organic carbon sources in soils of the Atacama Desert. Glob. Planet. Change 184, 103078. https://doi.org/10.1016/j.gloplacha.2019.103078.
Kolattukudy, P.E., 2001. Polyesters in higher plants. Adv. Biochem. Eng. /Biotechnol. 71, 1–49. https://doi.org/10.1007/3-540-40021-4_1.
Komada, T., Anderson, M.R., Dorfmeier, C.L., 2008. Carbonate removal from coastal sediments for the determination of organic carbon and its isotopic signatures, δ13C and Δ14C: comparison of fumigation and direct acidification by hydrochloric acid. Limnol. Oceanogr. Methods 6 (6), 254–262. https://doi.org/10.4319/lom.2008.6.254.
Lajtha, K., Bowden, R.D., Nadelhoffer, K., 2014. Litter and root manipulations provide insights into soil organic matter dynamics and stability. Soil Sci. Soc. Am. J. 78 (S1), S261–S269. https://doi.org/10.2136/sssaj2013.08.0370nafsc.
Langer, U., Rinklebe, J., 2009. Lipid biomarkers for assessment of microbial communities in floodplain soils of the Elbe River (Germany). Wetlands 29 (1), 353–362. https://doi.org/10.1672/08-114.1.
Li, F., Pan, B., Zhang, D., Yang, X., Li, H., Liao, S., Ghaffar, A., Peng, H., Xing, B., 2015. Organic matter source and degradation as revealed by molecular biomarkers in agricultural soils of Yuanyang terrace. Sci. Rep. 5 (1), 1–9. https://doi.org/10.1038/srep11074.
Li, J., Lv, L., Wang, R., Long, H., Yang, X., 2022. Spatial distribution of n-alkanes in the catchment and sediments of Lake Lugu, Southwest China: Implications for palaeoenvironment reconstruction. Palaeogeograp Palaeocli 592, 110895. https://doi.org/10.1016/j.palaeo.2022.110895.
Li, Y., Li, Z., Chang, S.X., Cui, S., Jagadamma, S., Zhang, Q., Cai, Y., 2020. Residue retention promotes soil carbon accumulation in minimum tillage systems: Implications for conservation agriculture. Sci. Total Environ. 740, 140147. https://doi.org/10.1016/j.scitotenv.2020.140147.
Lichtfouse, E., Leblond, C., Da Silva, M., Béhar, F., 1998. Occurrence of biomarkers and straight-chain biopolymers in humin: implication for the origin of soil organic matter. Die Nat. 85 (10), 449–452. https://doi.org/10.1007/s001140050538.
Ludwig, M., Achtenhagen, J., Miltner, A., Eckhardt, K.U., Leinweber, P., Emmerling, C., Thiele-Bruhn, S., 2015. Microbial contribution to SOM quantity and quality in density fractions of temperate arable soils. Soil Biol. Biochem 81, 311–322. https://doi.org/10.1016/j.soilbio.2014.12.002.
Lv, J., Huang, Z., Luo, L., Zhang, S., Wang, Y., 2022. Advances in Molecular and Microscale Characterization of Soil Organic Matter: Current Limitations and Future Prospects. Environ. Sci. Technol. 56 (18), 12793–12810. https://doi.org/10.1021/acs.est.2c00421.
Mendez-Millan, M., Dignac, M.F., Rumpel, C., Derenne, S., 2011. Can cutin and suberin biomarkers be used to trace shoot and root-derived organic matter? A molecular and isotopic approach. Biogeochemistry 106 (1), 23–38. https://doi.org/10.1007/s10533-010-9407-8.
Mendez-Millan, M., Dignac, M.F., Rumpel, C., Rasse, D.P., Bardoux, G., Derenne, S., 2012. Contribution of maize root derived C to soil organic carbon throughout an agricultural soil profile assessed by compound specific 13C analysis. Org. Geochem 42 (12), 1502–1511. https://doi.org/10.1016/j.orggeochem.2011.02.008.
Nierop, K.G., Naafs, D.F., Verstraten, J.M., 2003. Occurrence and distribution of ester-bound lipids in Dutch coastal dune soils along a pH gradient. Org. Geochem 34 (6), 719–729. https://doi.org/10.1016/S0146-6380(03)00042-1.
Nierop, K.G., van Bergen, P.F., Buurman, P., van Lagen, B., 2005. NaOH and Na4P2O7 extractable organic matter in two allophanic volcanic ash soils of the Azores Islands—a pyrolysis GC/MS study. Geoderma 127 (1-2), 36–51. https://doi.org/10.1007/978-3-540-48711-1_29.
Otto, A., Simoneit, B.R., Rember, W.C., 2005. Conifer and angiosperm biomarkers in clay sediments and fossil plants from the Miocene Clarkia Formation, Idaho, USA. Org. Geochem 36 (6), 907–922. https://doi.org/10.1016/j.orggeochem.2004.12.004.
Pancost, R.D., Baas, M., van Geel, B., Damsté, J.S.S., 2002. Biomarkers as proxies for plant inputs to peats: an example from a sub-boreal ombrotrophic bog. Org. Geochem 33 (7), 675–690. https://doi.org/10.1016/S0146-6380(02)00048-7.
Paterson, E., Gebbing, T., Abel, C., Sim, A., Telfer, G., 2007. Rhizodeposition shapes rhizosphere microbial community structure in organic soil. N. Phytol. 173 (3), 600–610. https://doi.org/10.1111/j.1469-8137.2006.01931.x.
Poynter, J., Eglinton, G., 1990. 14. Molecular composition of three sediments from hole 717c: The Bengal fan. Proc. Ocean Drill. Program. Sci. Results 116, 155–161. https://doi.org/10.1594/PANGAEA.756551.
Puglisi, E., Nicelli, M., Capri, E., Trevisan, M., Del Re, A.A., 2003. Cholesterol, β-sitosterol, ergosterol, and coprostanol in agricultural soils. J. Environ. Qual. 32 (2), 466–471. https://doi.org/10.2134/jeq2003.4660.
Quezada, M., Buitrón, G., Moreno-Andrade, I., Moreno, G., López-Marín, L.M., 2007. The use of fatty acid methyl esters as biomarkers to determine aerobic, facultatively aerobic and anaerobic communities in wastewater treatment systems. FEMS Microbiol. Lett. 266 (1), 75–82. https://doi.org/10.1111/j.1574-6968.2006.00509.x.
Rao, Z., Guo, W., Cao, J., Shi, F., Jiang, H., Li, C., 2017. Relationship between the stable carbon isotopic composition of modern plants and surface soils and climate: A global review. Earth Sci. Rev. 165, 110–119. https://doi.org/10.1016/j.earscirev.2016.12.007.
Reiffarth, D.G., Petticrew, E.L., Owens, P.N., Lobb, D.A., 2016. Sources of variability in fatty acid (FA) biomarkers in the application of compound-specific stable isotopes (CSSIs) to soil and sediment fingerprinting and tracing: a review. Sci. Total Environ. 565, 8–27. https://doi.org/10.1016/j.scitotenv.2016.04.137.
Ren, L., Fu, P., He, Y., Hou, J., Chen, J., Pavuluri, C.M., Sun, Y., Wang, Z., 2016. Molecular distributions and compound-specific stable carbon isotopic compositions of lipids in wintertime aerosols from Beijing. Sci. Rep. 6 (1), 1–12. https://doi.org/10.1038/srep27481.
Rieley, G., 1994. Derivatization of organic compounds prior to gas chromatographic–combustion–isotope ratio mass spectrometric analysis: identification of isotope fractionation processes. Analyst 119 (5), 915–919. https://doi.org/10.1039/AN9941900915.
Rielley, G., Collier, R.J., Jones, D.M., Eglinton, G., 1991. The biogeochemistry of Ellesmere Lake, UK—I: source correlation of leaf wax inputs to the sedimentary lipid record. Org. Geochem 17 (6), 901–912. https://doi.org/10.1016/0146-6380(91)90031-E.
Routh, J., Hugelius, G., Kuhry, P., Filley, T., Tillman, P.K., Becher, M., Crill, P., 2014. Multi-proxy study of soil organic matter dynamics in permafrost peat deposits reveal vulnerability to climate change in the European Russian Arctic. Chem. Geol. 368, 104–117. https://doi.org/10.1016/j.chemgeo.2013.12.022.
Rumpel, C., Eusterhues, K., Kögel-Knabner, I., 2004. Location and chemical composition of stabilized organic carbon in topsoil and subsoil horizons of two acid forest soils. Soil Biol. Biochem 36 (1), 177–190. https://doi.org/10.1016/j.soilbio.2003.09.005.
San-Emeterio, L.M., De la Rosa, J.M., Knicker, H., López-Núñez, R., González-Pérez, J.A., 2023b. Evolution of maize compost in a mediterranean agricultural soil: implications for carbon sequestration. Agronomy 13 (3), 769. https://doi.org/10.3390/agronomy13030769.
San-Emeterio, L.M., Jiménez-Morillo, N.T., Pérez-Ramos, I.M., Domínguez, M.T., González-Pérez, J.A., 2023a. Changes in soil organic matter molecular structure after five-years mimicking climate change scenarios in a Mediterranean savannah. Sci. Total Environ. 857, 159288. https://doi.org/10.1016/j.scitotenv.2022.159288.
Simoneit, B.R., Mazurek, M.A., 2007. Organic matter of the troposphere—II.: natural background of biogenic lipid matter in aerosols over the rural western United States. Atmos. Environ. 41, 4–24. https://doi.org/10.1016/j.atmosenv.2007.10.056.
Smith, C.J., Chalk, P.M., 2021. Carbon (δ13C) dynamics in agroecosystems under traditional and minimum tillage systems: a review. Soil Res 59, 661–672. https://doi.org/10.1071/SR21056.
Sokol, N.W., Bradford, M.A., 2019. Microbial formation of stable soil carbon is more efficient from belowground than aboveground input. Nat. Geosci. 12 (1), 46–53. https://doi.org/10.1038/s41561-018-0258-6.
Spielvogel, S., Prietzel, J., Leide, J., Riedel, M., Zemke, J., Kögel-Knabner, I., 2014. Distribution of cutin and suberin biomarkers under forest trees with different root systems. Plant Soil 381 (1), 95–110. https://doi.org/10.1007/s11104-014-2103-z.

Thomas, C.L., Jansen, B., van Loon, E.E., Wiesenberg, G.L., 2021. Transformation of n-alkanes from plant to soil: a review. Soil 7 (2), 785–809. https://doi.org/10.5194/soil-7-785-2021.

Tu, T.T.N., Egasse, C., Anquetil, C., Zanetti, F., Zeller, B., Huon, S., Derenne, S., 2017. Leaf lipid degradation in soils and surface sediments: A litterbag experiment. Org. Geochem 104, 35–41. https://doi.org/10.1016/j.orggeochem.2016.12.001.

Van Bergen, P.F., Bull, I.D., Poulton, P.R., Evershed, R.P., 1997. Organic geochemical studies of soils from the Rothamsted Classical Experiments—I. Total lipid extracts, solvent insoluble residues and humic acids from Broadbalk Wilderness. Org. Geochem 26 (1-2), 117–135. https://doi.org/10.1016/S0146-6380(96)00134-9.

Van Hees, P.A.W., Vinogradoff, S.I., Edwards, A.C., Godbold, D.L., Jones, D.L., 2003. Low molecular weight organic acid adsorption in forest soils: effects on soil solution concentrations and biodegradation rates. Soil Biol. Biochem 35 (8), 1015–1026. https://doi.org/10.1016/S0038-0717(03)00144-5.

Vanmierlo, T., Husche, C., Schött, H.F., Pettersson, H., Lütjohann, D., 2013. Plant sterol oxidation products–analogs to cholesterol oxidation products from plant origin? Biochimie 95 (3), 464–472. https://doi.org/10.1016/j.biochi.2012.09.021.

Verardo, D.J., Froelich, P.N., McIntyre, A., 1990. Determination of organic carbon and nitrogen in marine sediments using the Carlo Erba NA-1500 Analyzer. Deep Sea Res. Part A. 37 (1), 157–165. https://doi.org/10.1016/0198-0149(90)90034-S.

Wang, Y., Li, S., Xu, Y., Li, M., Shan, T., Zhang, W., Liu, X., Farhan-Saeed, M., Wang, J., 2020. Incorporated maize residues will induce more accumulation of new POC in HF compared with that in LF soils: a comparison of different residue types. J. Soils Sediment. 20 (11), 3941–3950. https://doi.org/10.1007/s11368-020-02718-9.

Wiesenberg, G.L., Schwarzbauer, J., Schmidt, M.W., Schwark, L., 2004. Source and turnover of organic matter in agricultural soils derived from n-alkane/n-carboxylic acid compositions and C-isotope signatures. Org. Geochem 35 (11-12), 1371–1393. https://doi.org/10.1016/j.orggeochem.2004.03.009.

Wiesenberg, G.L., Lehndorff, E., Schwark, L., 2009. Thermal degradation of rye and maize straw: lipid pattern changes as a function of temperature. Org. Geochem 40 (2), 167–174. https://doi.org/10.1016/j.orggeochem.2008.11.004.

Wiesenberg, G.L.B., 2004. Input and turnover of plant-derived lipids in arable soils. Doctoral dissertation. Universität zu Köln.

Wu, M.S., West, A.J., Feakins, S.J., 2019. Tropical soil profiles reveal the fate of plant wax biomarkers during soil storage. Org. Geochem 128, 1–15. https://doi.org/10.1016/j.orggeochem.2018.12.011.

Wynn, J.G., Bird, M.I., 2007. C4-derived soil organic carbon decomposes faster than its C3 counterpart in mixed C3/C4 soils. Glob. Change Biol. 13 (10), 2206–2217. https://doi.org/10.1111/j.1365-2486.2007.01435.x.

Xie, N., An, T., Zhuang, J., Radosevich, M., Schaeffer, S., Li, S., Wang, J., 2022. High initial soil organic matter level combined with aboveground plant residues increased microbial carbon use efficiency but accelerated soil priming effect. Biogeochemistry 160 (1), 1–15. https://doi.org/10.1007/s10533-022-00936-6.

Xie, S., Nott, C.J., Avsejs, L.A., Maddy, D., Chambers, F.M., Evershed, R.P., 2004. Molecular and isotopic stratigraphy in an ombrotrophic mire for paleoclimate reconstruction. Geochim. Cosmochim. Acta 68 (13), 2849–2862. https://doi.org/10.1016/j.gca.2003.08.025.

Yang, S., Jansen, B., Absalah, S., Kalbitz, K., Cammeraat, E.L., 2020. Selective stabilization of soil fatty acids related to their carbon chain length and presence of double bonds in the Peruvian Andes. Geoderma 373, 114414. https://doi.org/10.1016/j.geoderma.2020.114414.

Yu, G.H., Kuzyakov, Y., 2021. Fenton chemistry and reactive oxygen species in soil: Abiotic mechanisms of biotic processes, controls and consequences for carbon and nutrient cycling. Earth Sci. Rev. 214, 103525. https://doi.org/10.1016/j.earscirev.2021.103525.

Zelles, L., 1999. Fatty acid patterns of phospholipids and lipopolysaccharides in the characterisation of microbial communities in soil: a review. Biol. Fertil. Soils 29, 111–129. https://doi.org/10.1007/s003740050533.

Zelles, L., Bai, Q.Y., 1993. Fractionation of fatty acids derived from soil lipids by solid phase extraction and their quantitative analysis by GC-MS. Soil Biol. Biochem 25 (4), 495–507. https://doi.org/10.1016/0038-0717(93)90075-M.

Zeng, J., Li, X., Jian, J., Xing, L., Li, Y., Wang, X., Zhang, Q., Ren, C., Yang, G., Han, X., 2024. Differences in the regulation of soil carbon pool quality and stability by leaf-litter and root-litter decomposition. Environ. Res. 263, 120285. https://doi.org/10.1016/j.envres.2024.120285.

Zheng, Y., Zhou, W., Meyers, P.A., Xie, S., 2007. Lipid biomarkers in the Zoigê-Hongyuan peat deposit: Indicators of Holocene climate changes in West China. Org. Geochem 38 (11), 1927–1940. https://doi.org/10.1016/j.orggeochem.2007.06.012.